DESIGN, CONSTRUCTION, AND VALIDATION OF THE AFIT SMALL SCALE COMBUSTION FACILITY AND SECTIONAL MODEL OF THE ULTRA-COMPACT COMBUSTOR

THESIS

Wesly S. Anderson, Second Lieutenant, USAF

AFIT/GAE/ENY/07-M01

DEPARTMENT OF THE AIR FORCE
AIR UNIVERSITY
AIR FORCE INSTITUTE OF TECHNOLOGY

Wright-Patterson Air Force Base, Ohio

AFIT/GAE/ENY/07-M01

DESIGN, CONSTRUCTION, AND VALIDATION OF THE AFIT SMALL SCALE COMBUSTION FACILITY AND SECTIONAL MODEL OF THE ULTRA-COMPACT COMBUSTOR

THESIS

Presented to the Faculty

Department of Aeronautics and Astronautics

Graduate School of Engineering and Management

Air Force Institute of Technology

Air University

Air Education and Training Command

In Partial Fulfillment of the Requirements for the

Degree of Master of Science in Aeronautical Engineering

Wesly S. Anderson, BS

Second Lieutenant, USAF

March 2007

AFIT/GAE/ENY/07-M01

DESIGN, CONSTRUCTION, AND VALIDATION OF THE AFIT SMALL SCALE COMBUSTION FACILITY AND SECTIONAL MODEL OF THE ULTRA-COMPACT COMBUSTOR

Wesly S. Anderson, BS
Second Lieutenant, USAF

Approved:

Maj Richard Branam, USAF (Chairman) — date: 9 Mar 07

Lt Col Raymond Maple, USAF (Member) — date: 9 Mar 07

Dr. Mark Reeder (Member) — date: 9 Mar 07

AFIT/GAE/ENY/07-M01

Abstract

The AFIT small-scale combustion facility is complete and its first experiment designed and built. Beginning with the partially built facility, detailed designs have been developed to complete the laboratory in order to run small-scale combustion experiments at atmospheric pressure. A sectional model of the Ultra-Compact Combustor has also been designed and built. Although the lab's specific design intent was to study the UCC's cavity-vane interaction, facility flexibility has also been maintained for future work. The design enabled the completion of liquid fuel and air delivery systems, power and control systems, and test equipment. The design includes failsafe operation, remote control, and adherence to SAE ARP 1256 testing standards. Construction of the laboratory has forced design changes as new obstacles arose. As system construction has been completed validation and troubleshooting have been undertaken. The AFIT facility can now deliver air in two separately controlled air lines at up to 530 K (500 °F), at delivery rates of 0.12 kg/s (200 SCFM) for the main line and 0.03 kg/s (60 SCFM) for the secondary. A continuous dual syringe pump can deliver liquid fuel at up to 5.67 mL/s for JP-8 equivalence ratios up to 4. Safe, remote ignition and shutdown are in place and all test equipment fundamental to combustion is installed. The addition of an advanced laser combustion diagnostics system adds more unique capability to the laboratory. The laser system will provide instantaneous Raman and Raman spectroscopy, Coherent Anti-Stokes Raman Scattering, Planar Laser-Induced Fluorescence, Laser-Induced Incandescence and Planar Imaging Velocimetry diagnostic techniques.

Acknowledgements

I would like to thank my wife for handling her first few years of marriage in a new place and to a husband that is always working with such grace and show of support. I want to thank my parents for raising me how they did. My brother and I won't easily forget their lessons of, "If you are gonna do something, do it right," and a thousand others.

I would like to thank my advisor, Major Richard Branam, for taking me on mid-stride, providing direction and being so knowledgeable and approachable. I owe a thank you to my first advisor, Dr. Ralph Anthenien for his foresight and expertise. I am very thankful for Eric Dittman and his extra efforts on my behalf, and John Hixenbaugh for his technical know-how, approachability, effort, and attitude.

Thank you to my friends for making things easier to bear. Special thanks to Joshua Crouse, Tim Pitzer, Tim Booher, Erik Saladin and Barth Boyer for their extra support. Also, I would like to thank Ryan Carr for always being up for some fun and a run in the wildest places we could find in Ohio.

Finally, I owe everything to Jesus Christ, my refuge. It is all worthless apart from you. Soli Deo Gloria.

Wesly S. Anderson

Table of Contents

Page

Abstract iv

Acknowledgements v

Table of Contents vi

List of Figures viii

List of Tables xi

List of Symbols xii

List of Abbreviations xiii

I. .....Introduction 1

1.1 Research and Design Perspective 1

1.2 Description of the Ultra Compact Combustor 2

1.3 Objectives 4

1.4 Methods 5

II. .....Theory and Background 7

2.1 History of UCC Research 7

Standard Combustor Design 7

Inter-Stage Turbine Burning 8

Trapped Vortex Combustion 10

Centrifugally Loaded Combustion 11

Experimental Research on the UCC 11

Computational Fluid Dynamics Research on the UCC 13

2.2 2-D Sector Rig Design 14

2.3 Existing Experimental Facility and Intended Measurements 16

Emissions measurements 17

Mass Flow Measurement 22

Pressure Transducers and Thermocouples 23

2.4 Laser Diagnostic Systems 23

Instantaneous Raman and Raman Spectroscopy 23

Page

CARS 29
PLIF 32
LII 39
PIV 41

III.....Methodology 44
3.1 System Design and Operation 44
Computer Control and Data Acquisition 45
Data Acquisition and Control Software 47
Power supply systems 49
Combustor Rig Air 54
Fuel Supply 58
Remote Ignition 60
Nitrogen Purge 61
Gas Analyzer 64
Emissions Collection 65
Instrument Air 68
Combustor Stand 69
Exhaust System 70
Laser Diagnostic System 71
3.2 Real Combustor Design 72

IV. .....Results and Discussion 76

V.....Conclusions 79
5.1 Overview of Project 79
5.2 Future Work and Recommendations 80

Appendix A: System Technical Information 82

Appendix B: Operational Checklist for System Startup 94

Bibliography 96

List of Figures

Page

Figure 1: Orginial UCC experimental setup without RVC's. (Zelina, Sturgess and Shouse, 2004) 3

Figure 2: Detail of UCC with RVC's, this model was used in CFD research. (Greenwood, 2005:1-4) 3

Figure 3: Detail of air and fuel injection in the UCC. (Anthenien et al, 2001:6) 4

Figure 4: Standard combustor design (Wilson, 1998:528) 8

Figure 5: Engine cycle for a typical gas turbine (dashed) and those with turbine burning included (solid). (Sirignano and Liu, 2000:9) 8

Figure 6: The Trapped Vortex Combustion concept. (Greenwood, 2005:1-2)..... 10

Figure 7: Curved sectional 2-D rig used by Moenter for CFD comparisons of the final design. This plot shows contours of temperature (K). Airflow is to the right in the cavity and out of the page in the main vane. (Moenter, 2006: 112) 14

Figure 8: Comparison of the 2-D curved cavity rig used as the final curved 2-D sectional design (top) with the baseline configuration using boundary conditions to simulate a full 360 cavity (bottom). Cavity airflow is left to right in both cases; main airflow is out of the page. Velocity vectors are shown colored with temperature (K). The large eddy in the center of the field clearly shows the interaction of the RVC with the cavity flow. The large amount of air entrained into the room in the experimental rig is also shown. (Moenter 2006: 117)..... 16

Figure 9: Paramagnetic oxygen detector theory (Supplemental Oxygen Manual, Sec. 6:17-19) 19

Figure 10: Principle of operation of the paramagnetic oxygen detector (Supplemental Oxygen Manual, Sec. 6:17-19)..... 20

Figure 11: NDIR Analyzer for CO and CO_2 (Manual for Infrared Analyzers, Sec 2: 9) 21

Figure 12: Incoherent light scattering and resulting spectra. The upper diagram indicates two electronic energy states with vibrational energy levels. Upward arrows indicate increasing energy. Raman and Rayleigh scattering are shown. The symbol λ indicates signal wavelength. (Eckbreth, 1988:11)..... 25

Figure 13: Basic setup for a time averaged Raman measurement. CCD cameras are commonly in use today in place of photomultipliers. (Eckbreth, 1988:190) 29

Page

Figure 14: Example of dual-pump CARS experimental setup for N_2-CO_2 measurements. OSC is oscillator, AMP is amplifier, NBDL is a narrowband dye laser, BBDL is a broadband dye laser and the SPEX 1000M is a 1.0m spectrometer. (Roy, Meyer, Lucht, et al, 2005:22, used with permission) 32

Figure 15: Fluorescent absorption, emission and resulting spectra. The upper diagram indicates two electronic energy states with vibrational energy levels. Upward arrows indicate increasing energy. The symbol λ indicates signal wavelength. (Eckbreth, 1988:11) 34

Figure 16: Fluorescent absorption and emission spectra for the OH radical at 2000K and 1 atm in air. These plots were produced with the LIFBASE software. They show maximum absorption at nearly 283 nm and maximum emission at 309 nm. 37

Figure 17: Schematic of experimental setup for conducting simultaneous LII and OH PLIF measurements. The OH PLIF is provided by the pumped dye laser at 284 nm. (Meyer and Roy, 26:2003, used with permission)..... 38

Figure 18: California Analytical Instruments raw exhaust analyzer test bench (l) and laboratory computer control station (r). 44

Figure 19: Diagram of control systems connectivity. 45

Figure 20: Peripheral hardware what provides direct control of the laboratory systems by the CPU. 47

Figure 21: Combustion facility control software flow of operation. (Dittman, 2006:32) 49

Figure 22: AC Power wiring diagram. 51

Figure 23: DC power wiring diagram. 52

Figure 24: Power distribution and signal lines in pressure transducer boxes. 53

Figure 25: Rig airlines upstream of electric heaters. 54

Figure 26: Rig airflow control loop. 55

Figure 27: Signal line connection schematic of rig air control loop and data transmission. 56

Figure 28: Heater emergency shutoff and data transmission. 58

Figure 29: Liquid fuel pump and control system 59

Figure 30: ISCO fuel pump system. 60

Figure 31: Solenoid valves controlling ignition and purge systems and their connection to the combustor stand. 61

Figure 32: Liquid and gas systems in the laboratory. 63

Page

Figure 33: Oil heated emissions probe and electrically heated line on test stand..... 66

Figure 34: Mokon heater and pump unit for heat transfer oil used to cool emissions probe. 67

Figure 35: Temperature control loop of exposed emissions line. 68

Figure 36: Combustor stand with exhaust probe assembly. 70

Figure 37: Flat combustor cavity design with main vane. Airflow direction is shown in red. 72

Figure 38: Cross-section of curved combustor cavity. Airflow is shown in red; fuel flow is shown in blue. The location of airflow through the main vane (moving into the page) and the radial vane cavity (RVC) is also indicated. 73

List of Tables

Page

Table 1: Fundamental vibrational frequencies of selected molecules of interest. The vibrational frequencies represent the Stokes shift of the incident light for Raman techniques. 26

Table 2: Major allowed electronic transitions for species of interest . These transitions represent the bands active to fluorescent absorption. (Eckbreth, 1979:260-265) 36

Table 3: Ranges for gases analyzed by CAI test bench. 65

Table 4: Wiring code for NI SCXI 1100 DAQ measurement and control system. 82

Table 5: Wiring code for Opto 22 PB24 solid state relay board used for control of systems throughout the room. 85

Table 6: Wiring and digital channel code for Opto 22 G4PB24 optically isolated solid-state relay board used for controlling range selection on the raw emissions test bench. 86

Table 7: Type, concentration and connection for all laboratory gases. 87

Table 8: Compiled list of major equipment and technical data by system. 88

List of Symbols

Symbol	
C_2	Diatomic carbon
CH_4	Methane
CO	Carbon Monoxide
CO_2	Carbon Dioxide
C_2H_2	Acetylene
C_2H_4	Ethylene
g	Gravitational constant
h	Water content
H_C	Heat of combustion of fuel
H_2O	Water
k	Turbulent kinetic energy
M	Molecular Mass
Na	Sodium
N_2	Nitrogen
NO	Nitric Oxide
NO_X	Oxides of Nitrogen
NO_2	Nitrogen Dioxide
OH	Hydroxide
O_2	Oxygen
S_B	Buoyant flame speed
X	Molar fraction air to fuel
x	Number of carbon atoms, undefined quantity
y	Number of hydrogen atoms
Z	Constituent Z
α	Ratio of hydrogen to carbon atoms
ε	Rate of turbulent kinetic energy dissipation
η_b	Combustion efficiency %

List of Abbreviations

Abbreviation	
AC	Alternating current
AFIT	Air Force Institute of Technology
AFRL	Air Force Research Laboratory
ARP	Aerospace Recommended Practice
CAI	California Analytical Insturments
CARS	Coherent Anti-Stokes Raman Spectroscopy
CCD	Charge coupled device
CFD	Computational Fluid Dynamics
CPU	Central Processing Unit
CTB	Continuous turbine burner
DAQ	Data acquisition
DC	Direct current
EI	Emissions Index
FID	Flame ionization detector
HCLD	Heated chemiluminescent detection
HID	High image density
I/O	Input/output
IGV	Inlet guide vanes
ISSI	Innovative Scientific Solutions Inc.
ITB	Inter-stage turbine burner
LDV	Laser Doppler Velocimetry
LID	Low image density
LII	Laser-Induced Incandescence
LSV	Laser speckle Velocimetry
mA	milli-Amps
NDIR	Non-dispersive infrared
Nd:YAG	Neodymium-doped yttrium aluminium garnet
NI	National Instruments

nm	nanometer
PAH	Polycylic aromatic hydrocarbons
PC	Personal computer
PID	Proportional-integral-derivative
PIV	Particle Imaging Velocimetry
PLIF	Planar Laser Induced Fluorescence
ppm	Parts per million
PRV	Pressure reducing valve
RNG	Renormalization group theory
RVC	Radial Vane Cavity
SAE	Society of Automotive Engineers
SCFM	Standard cubic feet per minute
SCXI	Signal Conditioning Extension for Instrumentation
SSR	Solid state relay
ST	Specific thrust
TSFC	Thrust specific fuel consumption
TVC	Trapped Vortex Combustion
UCC	Ultra Compact Combustor
USB	Universal Serial Bus
VAC	Volts alternating current
VDC	Volts direct current
VI	Virtual Instrument
2-D	Two dimensional
3-D	Three dimensional

DESIGN, CONSTRUCTION, AND VALIDATION OF THE AFIT SMALL SCALE COMBUSTION FACILITY AND SECTIONAL MODEL OF THE ULTRA-COMPACT COMBUSTOR

I. Introduction

1.1 Research and Design Perspective

Efficient use of energy has always been highly desirable and this is true more today than ever. The cost of energy in terms of economic and environmental impact is being felt more and more as the world's demand increases. The Department of Defense requires enormous amounts of fuel for all of its endeavors. The vast majority of this goes to air operations. Increasing demand for energy from the Air Force and the world is not going away anytime soon, so better technology is the best and only answer to this problem. In the case of aircraft operations, improvements in turbine engine cycle performance can provide significant steps in the right direction.

The Ultra Compact Combustor (UCC) may be a partial solution for this problem. By making significant changes in airflow direction and fuel mixing in the combustor, the UCC will greatly reduce the axial length required for efficient combustion in a gas-turbine engine. This has the potential for two major advantages: First, advanced engine concepts such as inter-stage turbine burners (ITB) to improve thermodynamic cycle efficiencies may be utilized. Secondly, the UCC may be used as a standard combustor positioned between the compressor and turbine, reducing the weight and length of the engine. (Anthenien et al, 2001)

Previous experiments and Computational Fluid Dynamics (CFD) studies have been conducted on variations of the UCC design with promising results. However, due to geometry constraints no one has been able to directly study the flow field and combustion

inside much of the UCC. In order to do this it was necessary to build a sectional model and find an associated laboratory facility to provide the necessary diagnostics. It was determined that a new testing facility at the Air Force Institute of Technology (AFIT) would be constructed to investigate the cavity-vane interactions of the UCC sectional models and provide future combustion test capability for AFIT.

1.2 Description of the Ultra Compact Combustor

The full UCC (shown in Figure 2) is a product of research at the US Air Force Research Laboratory (AFRL), Propulsion Directorate at Wright-Patterson Air Force Base in Dayton, Ohio. Inspiration for the combustor came from a paper written by researchers at the University of California, Irvine demonstrating the use of inter-stage turbine burners (ITB) to significantly improve major engine performance measurements.

The combustor consists of an annular main flow around a blunt body positioned along the axial direction. A cavity surrounds this body running circumferentially around the main flow as shown in Figure 1. The cavity provides the main mixing and combustion region. The air-fuel mixture travels around this cavity providing necessary residence time for combustion without significant axial length. Air is injected into the cavity through 24 jets in the outer wall of the cavity. These jets are angled away from radial direction to provide swirling as shown in Figure 3. This jet swirling, along with the circumferential motion of the mixture through the cavity vane increases the flame speed. Fuel injects through an atomizer into six recessed chambers, utilizing trapped vortex combustion (TVC) to stabilize the flame and improve combustion efficiency.

The cavity vane is open to the axial main flow of air through the combustor. Six evenly spaced, radially extending airfoils hold the annular blunt body in place. These

airfoils also simulate inlet guide vanes (IGV) or stator blades, envisioning the use of the UCC as an ITB in the future. In order to provide for mass transport from the cavity flow to the main flow, radial vane cavities (RVC) are cut into the airfoil blades. This creates an intermediate combustion zone and provides a pressure gradient, drawing mass from the cavity vane into the main vane flow stream. A shown in Figure 3 the six fuel injection points are located directly over the RVC's and the 24 air injection jets are evenly spaced between the fuel injectors.

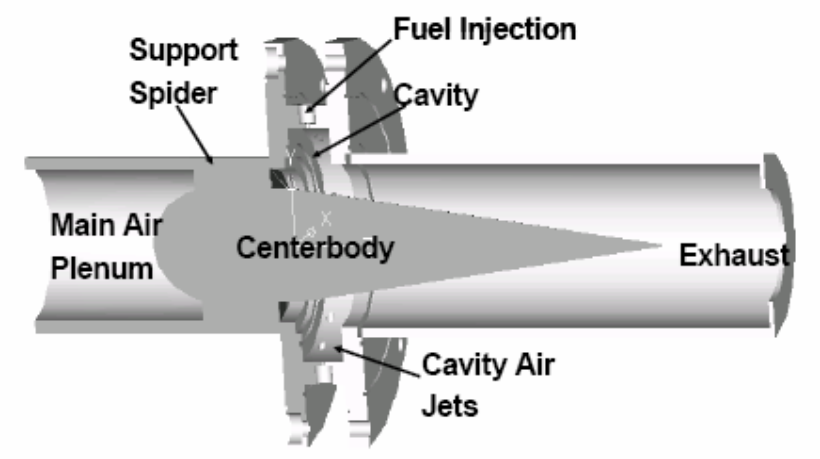

Figure 1: Orginial UCC experimental setup without RVC's. (Zelina, Sturgess and Shouse, 2004)

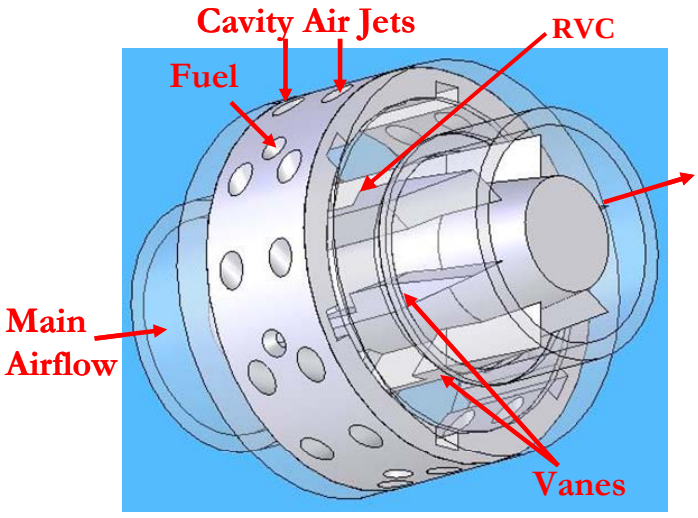

Figure 2: Detail of UCC with RVC's, this model was used in CFD research. (Greenwood, 2005:1-4)

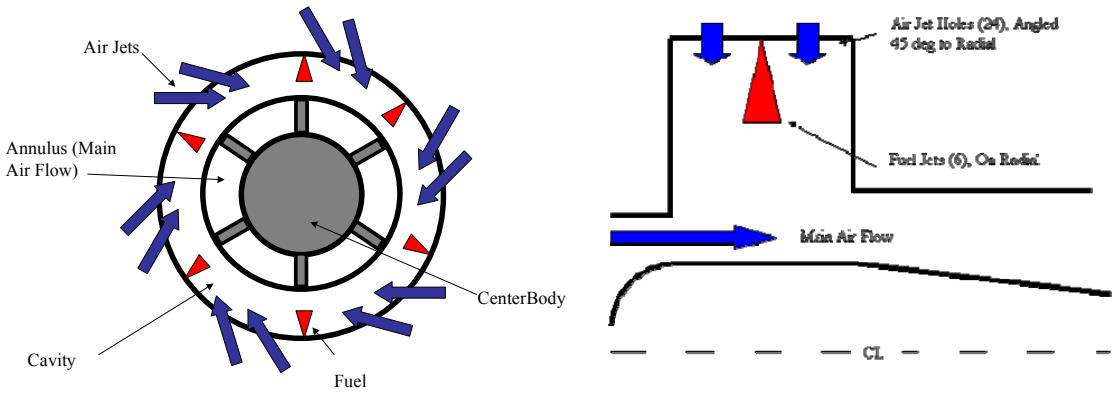

Figure 3: Detail of air and fuel injection in the UCC. (Anthenien et al, 2001:6)

1.3 Objectives

Construction of the AFIT small-scale combustion facility began in 2005 in building 641 room 258 under the direction of Dr. Ralph Anthenien and the efforts of Lt. Eric Dittman. At the completion of Lt. Dittman's work most of the major components of the facility were selected and in place. Also, a general plan for the integration of these components into a system had been developed, and much construction had been undertaken.

The facility was primarily intended to study the UCC cavity-vane interaction. However, as AFIT's first combustion facility it would also need to be expandable for future experiments. Safe, centralized control of the process through a computer station increases manageability of such a complex and potentially dangerous system. This station also allows for automated recording of data for accuracy and repeatability. Emissions analysis provides valuable information by using a gas analyzer and samples taken from the test section. Liquid fuel and heated air are provided in a controlled manner producing equivalence ratios between 0.2 and 4 at flows of 0.1 to 0.3 Mach at

low pressures in the test section (Dittman, 2006: 2). Safety systems allow safe operation to be observed at all times. Finally, ready access for laser diagnostics is provided by the final installation of a laser diagnostics system.

At the beginning of the author's work, many of the specific details of the facility design were undetermined, and much construction still needed to be accomplished, along with an overall evaluation of the systems functionality. Also, calibration, operational procedures and repair documentation needed to be developed. Finally, a sectional UCC rig needed to be designed and built to provide the facility with its first experiment and fulfill its original intent.

1.4 Methods

To complete the facility and accomplish all the previous goals several steps were undertaken:

1) *Study of existing project objectives and design.* It was necessary to understand the full intent of the project and the intent of the original facility design in order to begin the completion of the facility. A good working knowledge of the particular pieces was also necessary. In addition, previous CFD studies and work on the UCC needed to be well understood in order to work on the sectional UCC rigs.

2) *Assessment of project progress, system by system*. To develop a to-do list the project's actual progress needed to be understood in detail. For example, approximately half of the signal wiring from various instruments had been run to the computer station. It thus became necessary to know what particular signals were necessary and still needed to be constructed. Similar scenarios existed in many of the sub-systems.

3) *Design or re-design of systems.* Although general plans were often in place, specifics of a system design or its integration often were not. Detailed questions needed answering, such as: what type of valve would work best, or what materials are compatible with a particular gas? Also, the addition of systems with no existing plans made it necessary to begin new designs from the ground up.

4) *Purchase of necessary parts to complete design*. Selection and purchase of parts was a major effort of this project. This was often concurrent with the final design of the system as most of the pieces for the design were off-the-shelf.

5) *Construction and troubleshooting.* Construction often provided its own unique challenges, forcing on-the-spot redesign and creative solutions. This project has re-enforced the lesson that "the devil is in the details" as many design and construction challenges remained even with a good plan and major infrastructure in place.

II. Theory and Background

2.1 History of UCC Research

Standard Combustor Design

A standard combustor in most modern gas turbines uses some variation of the combustor can, or flame tube, concept. As seen in Figure 4 this type of combustor uses fuel injection along the axial direction of the engine in the center of the combustion can. Air enters the can from the compressor through turning vanes positioned around the fuel injection point or multiple holes in the can's side. Air entry is in two zones. A primary zone provides near stoichiometric air for combustion and forces flow patterns for mixing. The secondary (dilution) zone adds the remaining air to the mixture, cooling the gas and providing an even temperature profile so it can safely enter the turbine (Wilson, 1998: 528). This standard combustor design relies almost entirely on axial length to provide residence time for combustion. It causes significant pressure loss, as the axial flow must decelerate for combustion to occur. It is also fixed in-between the compressor and turbine of an engine and it thus limits possible variations of the engine's thermodynamic cycle.

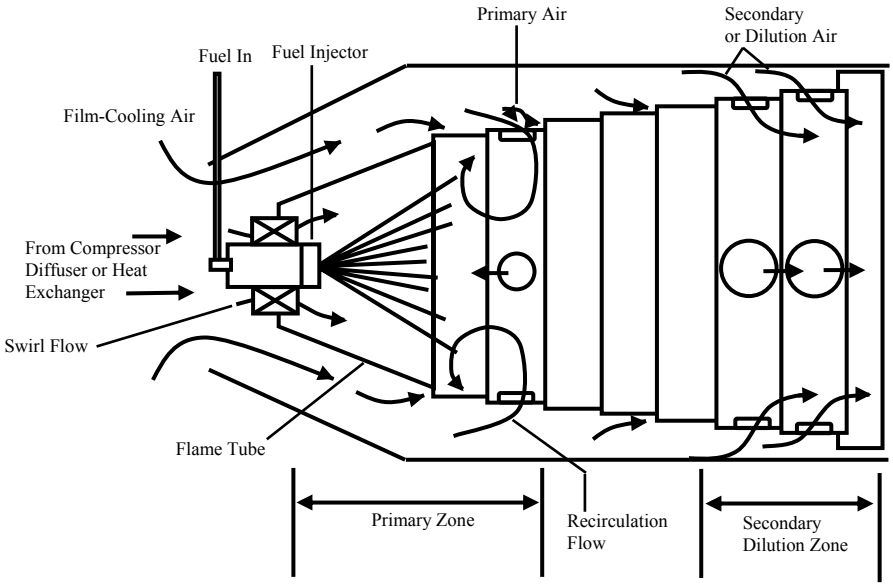

Figure 4: Standard combustor design (Wilson, 1998:528)

Inter-Stage Turbine Burning

In 1999 Sirignano and Liu proposed a concept that would significantly improve the efficiency of this gas turbine engine cycle. Figure 5 shows the T-S diagram for the major types of cycles studied.

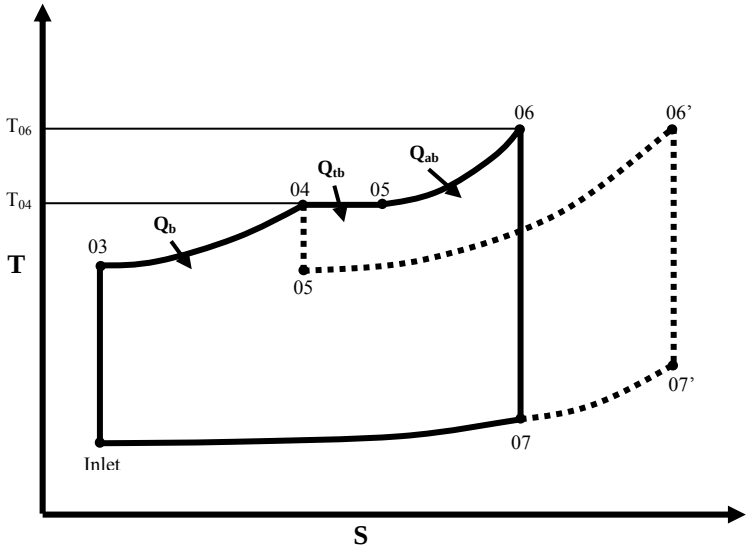

Figure 5: Engine cycle for a typical gas turbine (dashed) and those with turbine burning included (solid). (Sirignano and Liu, 2000:9)

As one can see, addition of heat in the turbine can add a considerable amount of energy to the cycle while remaining under the critical temperature limits of the turbine blades. Using this concept on many types of gas turbine cycles, Sirgnano and Liu found that use of a continuous turbine burner (CTB) would improve both the major engine performance parameters: Specific thrust (ST) would increase dramatically with only slight increases in thrust specific fuel consumption (TSFC). Using a CTB model, they report an improvement in ST of up to 50% with little or no change in TSFC on a turbofan engine (Sirignano and Liu, 1999:8). However, early in their paper the researchers admit the inherent difficulty of burning in a rotor stage of the turbine, and instead focus their efforts on the more practical use of inter-stage turbine burners (ITB's). These ITB's would ideally burn in the stator stages throughout the turbine. This design provides a more practical way to approach the desirable performance of the CTB.

The advantages of an ITB engine over a conventional design are obvious; however, stator burning is still a very difficult proposition. The most significant issue is the large axial length necessary in a standard combustor to provide for adequate residence time to efficiently mix and burn fuel. This is many times longer than the typical stator stage.

The Ultra Compact Combustor (UCC) provides a solution to the problem of residence time in a stator. The literature states that this combustor may be used as either a standard burner at the inlet guide vanes (IGV) of the turbine or an ITB. In either case, it would reduce the length of the engine significantly, resulting in weight savings. If used as an ITB it would significantly improve the cycle efficiency.

The UCC uses two major combustion concepts in an effort to burn fuel efficiently over a short axial length: Trapped vortex combustion (TVC) and use of centrifugal-force effects to increase flame speeds.

Trapped Vortex Combustion

TVC involves the use a recessed cavity. Inside this cavity a trapped vortex is generated by injecting fuel and air in such a way as to reinforce vortex motion. Figure 6 shows a TVC cavity and the direction of main airflow. When sized correctly this trapped vortex provides a stable region of flame igniting incoming air and fuel. Achieveing good mixing into the main cavity would allow the TVC to reduce NO_X emissions and improve combustion efficiencies. This stable, recessed flame would also allow for improved lean-blow-out, and good altitude relight capability. Thus, this design allows higher velocities to be achieved outside the TVC cavity while maintaining stable, efficient combustion (Roquemore et al, 2001). The UCC uses this concept at every location of its fuel injectors along the outside of the cavity vane running circumferentially around the engine.

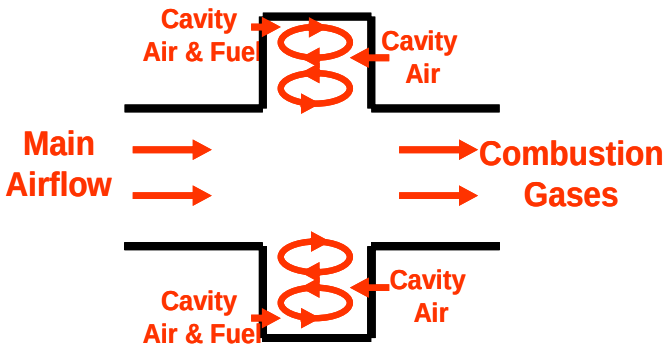

Figure 6: The Trapped Vortex Combustion concept. (Greenwood, 2005:1-2).

Centrifugally Loaded Combustion

Centrifugal loading of a combusting mixture increases flame speed dramatically due to buoyancy effects acting on less dense flame regions. Lewis empirically found buoyant bubble flame speed is often faster than either laminar or turbulent flame speeds in a centrifugally loaded mixture. He determined a relationship between the g-loading and this buoyant flame speed (S_B) applying for g-loads between 500 and 3500 (Lewis, 1973:2).

$$S_B = 1.25(g)^{\frac{1}{2}} \qquad (1)$$

Building off this concept, Yonezawa, et al. studied a jet swirled combustor. They employed g loading in their design by inclining the combustor air inlets to produce a ring of swirling vortexes. They showed high combustion efficiency could be attained with high combustion loading by use of this jet swirled design (Yonezawa et al, 1990).

In the UCC both of these concepts are incorporated in the cavity vane. Inside the cavity, the circumference of the engine is utilized to provide length for burning and curvature provides g loading for improved flame speed. In addition, air is injected into the cavity by off-axis jets providing swirling as in the jet swirled combustor.

Experimental Research on the UCC

Much experimental work has been conducted, and is currently underway, on the UCC by AFRL and others since 2001. Anthenien, et al studied the effects of varying equivalence ratios on a fixed geometry in a UCC rig at atmospheric pressure conditions. In these experiments, the main mass flow was almost four times the cavity air. These

experiments used JP-8 and ethanol fuels over a large range of operating conditions. Significantly shorter flame lengths were observed as compared to a standard, swirl stabilized combustor. High efficiencies of +99% were achieved up to cavity equivalence ratios greater than 2 and lean blowout was found down to a cavity equivalence ratio of 0.5 (Anthenien et al, 2001).

Zelina et al in 2001 also conducted studies into the effect of fuel injection method and angle. They found fuel injector type and angle greatly affected the UCC's combustion efficiency. From the data, they proposed two modes of operation. For low loadings, the flame seemed to be injector-stabilized. At higher loadings, the flame was bulk-flow stabilized. They found the combustor had stable and efficient operation with little pressure drop (2%). Finally, they noted increased g loading improved combustion efficiency by creating high radial turbulence in the cavity. (Zelina, et al, 2001)

Laser Doppler Velocimeter (LDV) experiments on the UCC found circumferential velocities of 20-45 m/s with accelerations of 1000-4000g in the cavity. Quaale et al compared these results to CFD models and found good agreement. These experiments found the cavity velocities were insensitive to the main flow velocity. Again, combustion efficiencies increased with g-loading, while residence time decreased. This increase in g loading also increased the CO Emission Index (Quaale et al, 2003).

Higher pressure rigs (Zelina, Shouse, and Neuroth, 2005) and the incorporation of the RVC (Radial Vane Cavity) (Zelina, Sturgess, and Shouse, 2004) were also introduced in several other experiments. These continued to show promise as the UCC performed well. Work continues today with the introduction of changes based on previous experiments and CFD research.

Computational Fluid Dynamics Research on the UCC

AFRL researchers and previous AFIT students have also conducted computational fluid dynamics (CFD) studies to examine the mixing and combustion inside the UCC. The AFIT work was begun by Greenwood using the commercial software FLUENT and standard k-ε turbulence models with second order, implicit solvers for steady state solutions. Greenwood first developed the proper heat transfer and fuel injection models and made a comparison of a one-sixth sector model of the combustor to experimental data from AFRL for the full UCC rig. He also studied changes in the geometry of the cavity (Greenwood, 2005). Anisko continued this work by improving periodic boundaries to include fuel particles, and investigations of further geometric variations (Anisko, 2006).

Moenter built on this work but used a model based on a statistical technique known as renormalization group theory (RNG). This RNG k-ε model was intended to provide greater accuracy and reliability than previous models. Moenter also corrected some mistakes from previous research. Notably he found pressure boundary conditions used incorrectly in Greenwood and Anisko's work. He then evaluated several numerical models at three cases of pressure and mass flow rates to develop both a 2-D flat and curved cavity rig expected to closely behave like the entire UCC in a one-sixth (60°) model. He soon found that a larger section of one-third (120°) was necessary. The combustor's behavior was compared to experiment based on the examination of velocity, temperature and other properties of the flow field at pre-defined locations to give a quantitative measurement. Also, measurements such as efficiency, emissions,

temperature distribution and pressure loss across the combustor were used as a qualitative basis of comparison (Moenter, 2006).

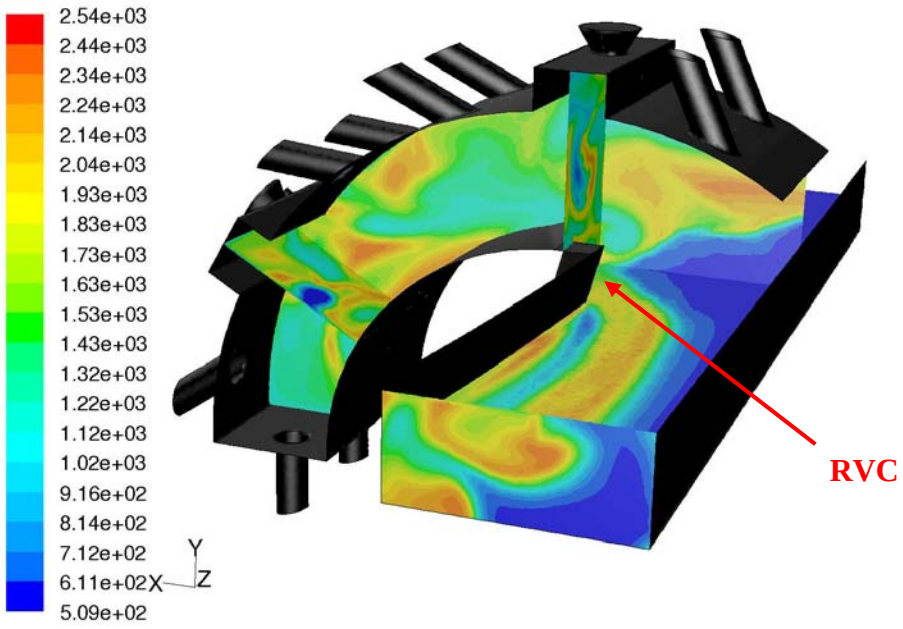

Figure 7: Curved sectional 2-D rig used by Moenter for CFD comparisons of the final design. This plot shows contours of temperature (K). Airflow is to the right in the cavity and out of the page in the main vane. (Moenter, 2006: 112)

2.2 2-D Sector Rig Design

The purpose of these new sector rig CFD models created by Moenter was to design real experimental 2-D flow rigs allowing greater optical access to study flow patterns and combustion in the UCC. Also, the creation of both a flat and curved cavity combustor would allow for empirical study into the effect of centrifugal loading on the combustor's performance.

Specifically, it was determined the flow behavior of the RVC and its wake were of interest and no good access could be gained with existing full (360°) UCC rigs. To simulate this cavity-vane interaction on a sectional rig allowing optical access, Moenter

found the most important areas to be reproduced were of the circumferential flow over the axial vane (representing a stator vane) and the main flow approaching this area.

Extra mass flow into the cavity was necessary in order to properly account for the mass entrained in the full combustor. As Figure 7 shows, two 60° segments, each with a fuel injection point, were deemed necessary to provide similar combustion behavior at the RVC. Additional air inlets at the cavity start provided the proper local equivalence ratio at the first fuel injection point. The main flow cavity was squared to provide useful optical access to the RVC. The design was then simplified by imbedding half the axial vane in a side wall not used for viewing and adjusting the geometry of the rig accordingly (Moenter, 2006:36). The size of the design was also reduced to one-sixth of the original UCC in order to match airflow capabilities of the experimental facility (Dittman, 2006: 17).

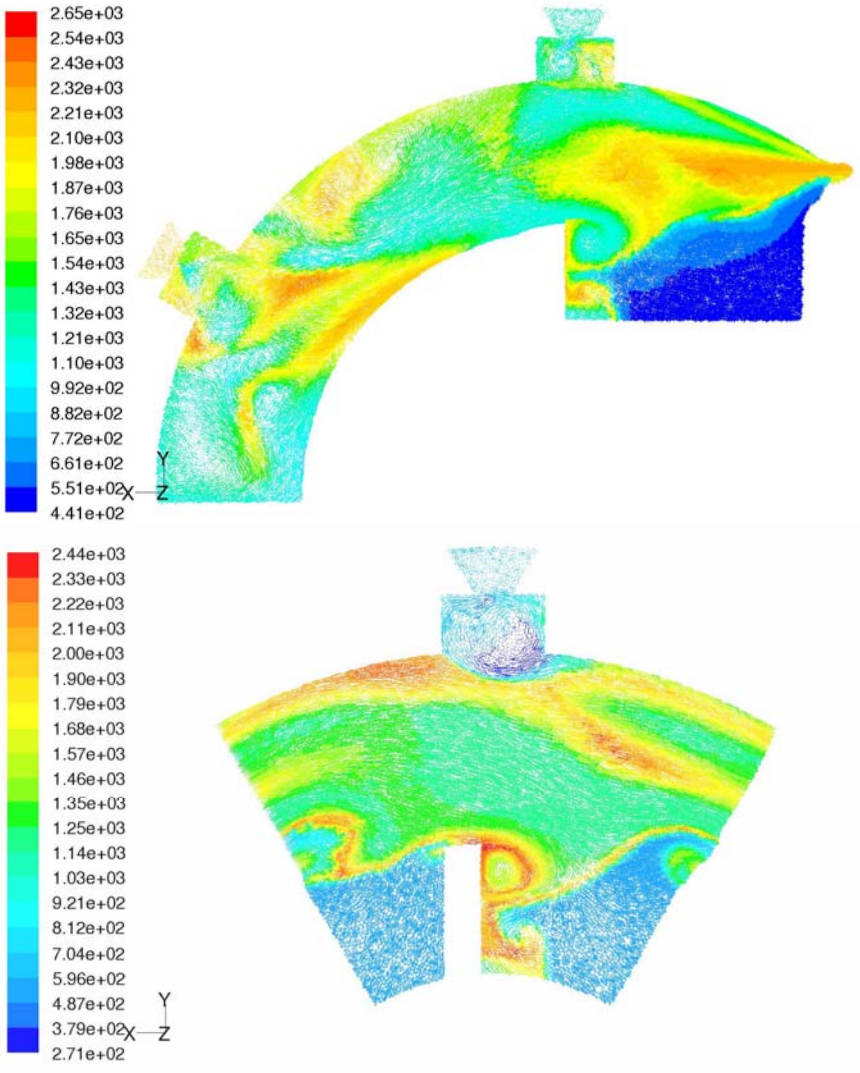

Figure 8: Comparison of the 2-D curved cavity rig used as the final curved 2-D sectional design (top) with the baseline configuration using boundary conditions to simulate a full 360 cavity (bottom). Cavity airflow is left to right in both cases; main airflow is out of the page. Velocity vectors are shown colored with temperature (K). The large eddy in the center of the field clearly shows the interaction of the RVC with the cavity flow. The large amount of air entrained into the room in the experimental rig is also shown. (Moenter 2006: 117)

2.3 Existing Experimental Facility and Intended Measurements

In order to generate useful information from any combustion experiment performed on the UCC it is necessary to measure several quantities considered fundamental to any combustion test facility. With the addition of laser diagnostics, the

facility can take necessary measurements on the UCC 2-D sectional rig as proposed. Thus, the facility can also provide more advanced experiments for any suitable combustion device. This section will examine these measurement techniques.

Emissions measurements

One of the fundamental quantities of interest is the emissions index (EI) of major combustion products. In general the emissions index (as defined in SAE ARP 1533: Section A1) is as follows:

$$EI_x = \frac{\text{Moles of Pollutant}}{\text{Moles of Fuel}} * \frac{\text{Molecular Weight of Pollutant}}{\text{Molecular Weight of Fuel}} * (1000) \qquad (2)$$

The emissions index is useful in calculating the efficiency of the combustor. Combustion efficiency gives an indication of how well the energy contained in fuel converts into heat addition to the air traveling through the combustor. According to the SAE standards, this can be calculated by the following:

$$\eta_b = \left[1.00 - 4.346 \frac{EI_{CO}}{H_C} - \frac{EI_{C_xH_y}}{1000} \right] (100) \qquad (3)$$

Where H_C is the heat of combustion of the fuel and η_b is the efficiency in percent. EI_{CO} and EI_{CxHy} are defined as:

$$EI_{CO} = \frac{[CO]}{[CO] + [CO_2] + [C_xH_y]} \frac{10^3 M_{CO}}{M_C + \alpha M_H} [1 + T(X/m)] \qquad (4)$$

$$EI_{C_xH_y} = \frac{\left[C_xH_y\right]}{\left[CO\right]+\left[CO_2\right]+\left[C_xH_y\right]} \frac{10^3 M_{C_xH_y}}{M_C + \alpha M_H}\left[1+T(X/m)\right] \tag{5}$$

Here [ ] indicates the concentration of the molecule enclosed. M represents the molecular weight and α is the ratio y/x. T is the molecular fraction of carbon dioxide in air. Its value is assumed to be 0.00034. X/m is defined as:

$$\left[X/m\right] = \frac{2Z-\alpha}{4(1+h-TZ/2)} \tag{6}$$

Where X is the molar fraction of air to fuel. The value h is the water content of the inlet air. Also, Z is defined as:

$$Z = \frac{2-\left[CO\right]-\left(\frac{2}{x}-\frac{y}{2x}\right)\left[C_xH_y\right]+\left[NO_2\right]}{\left[CO\right]+\left[CO_2\right]+\left[C_xH_y\right]} \tag{7}$$

The AFIT facility uses a probe to capture emissions from a combustion device such as the UCC. Gases entering the probe are then pumped to several sensors, combined into a single gas analyzer unit. The sensors in the unit are used to measure the concentrations of important combustion products and thus calculate the Emissions Index of that product. The gas analyzer measures total hydrocarbons, nitric oxide, carbon monoxide, carbon dioxide and oxygen concentrations in emission gases and meets SAE ARP 1256 standards for accuracy (Dittman, 2006:24).

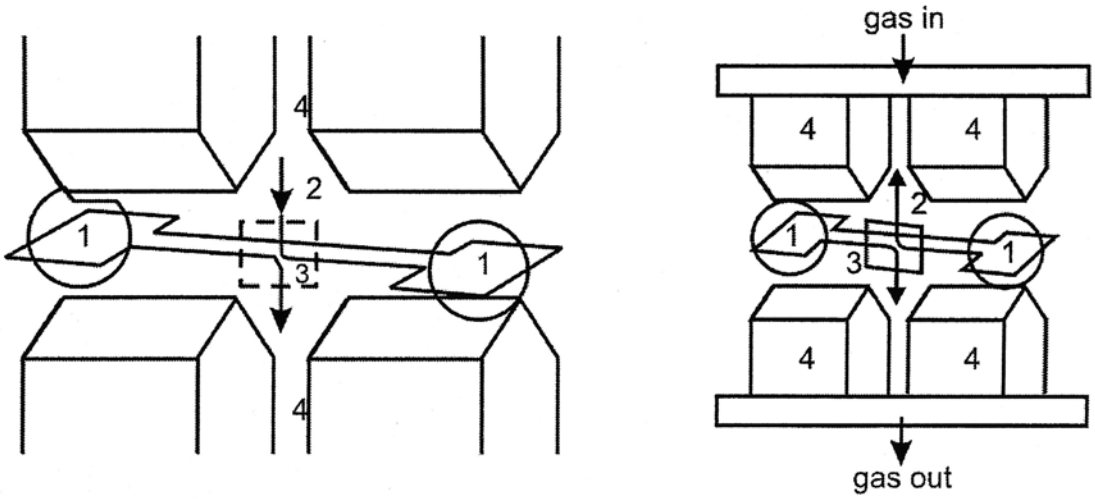

1 quartz spheres dumb-bell
2 platinum feedback coil
3 mirror
4 magnet pole pieces

Figure 9: Paramagnetic oxygen detector theory (Supplemental Oxygen Manual, Sec. 6:17-19)

A paramagnetic oxygen detector measures oxygen collected by the probe. This device takes advantage of oxygen's unique attraction to magnetic fields and nitrogen's repellence. As seen in Figure 9, two nitrogen filled quartz spheres are connected and suspended in a magnetic field. The field changes in the presence of oxygen as the emissions sample moves through the sensor. Repulsion of the nitrogen to the modified field results in a torque on the quartz dumbbell related to oxygen concentration. A mirror attached to the quartz dumbbell and a photocell provides greater refinement of this measurement. Light reflected off the mirror converts to an electrical signal by the photocells on each side of the dumbbell. As shown in Figure 10, this signal is amplified in a feedback loop and used to produce a magnetic field acting to restore the dumbbell position. The feedback loop also incorporates a temperature correction. (Supplemental Oxygen Manual, Sec. 6:17)

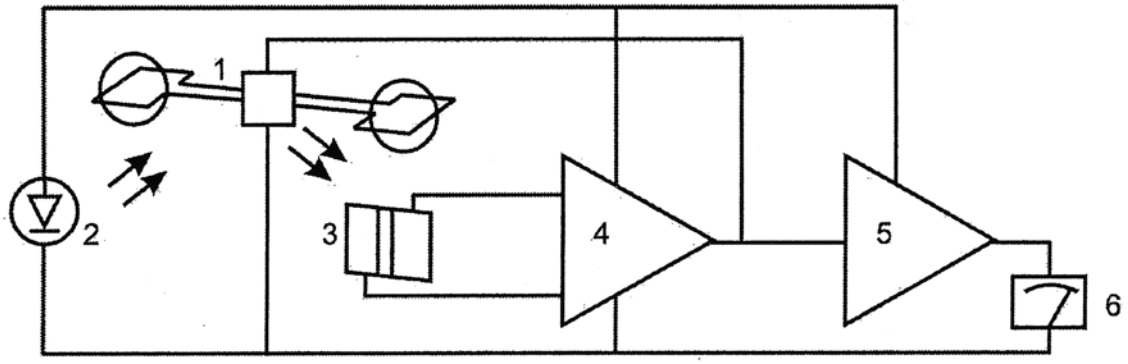

1 measuring cell
2 "led" light beam
3 photo cell
4 feedback amplifier
5 output amplifier
6 meter indication

Figure 10: Principle of operation of the paramagnetic oxygen detector (Supplemental Oxygen Manual, Sec. 6:17-19)

A Non-Dispersive Infrared (NDIR) sensor measures carbon monoxide and carbon dioxide. As shown in Figure 11 the sample gas is exposed in a circulating sample cell to infrared light modulating at a regular frequency by a chopper blade. The detector then absorbs residual light. The detector consists of pure CO or pure CO_2 in two chambers. Absorption of differing amounts of energy from the infrared light by the gas in the detector causes a pressure difference across the two chambers; this is measured by a micro flow sensor. This pressure difference relates to the amount of carbon monoxide present in the sample. (Operation and Maintenance Manual for Infrared Analyzers, Sec 2: 9-10)

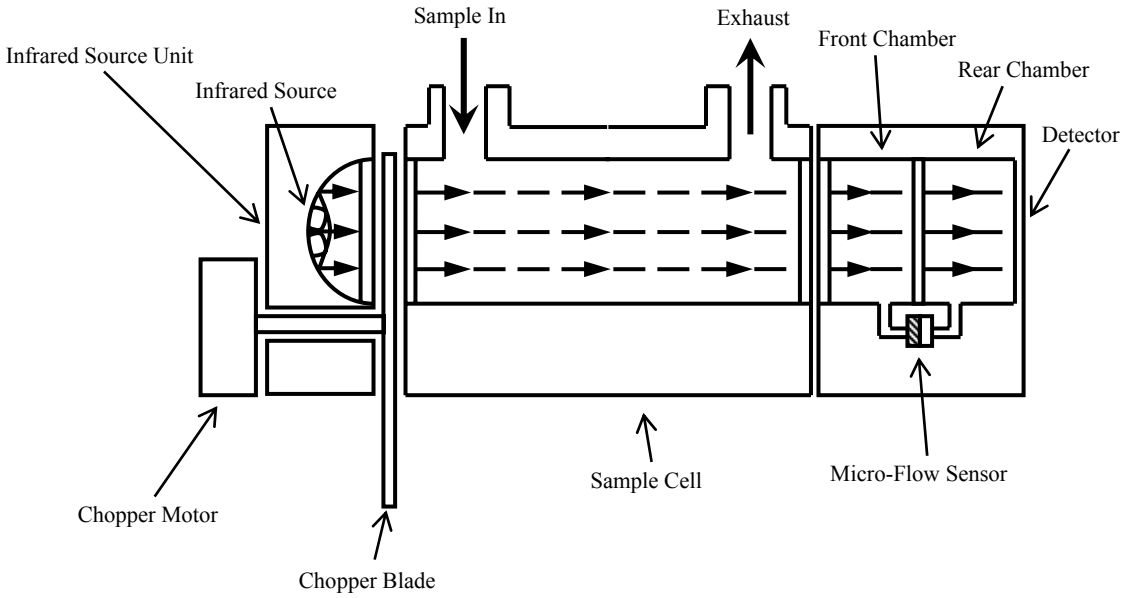

Figure 11: NDIR Analyzer for CO and CO_2 (Manual for Infrared Analyzers, Sec 2: 9)

A heated chemiluminescent detection (HCLD) sensor measures oxides of nitrogen. This sensor has two modes. In the NO mode, it first converts all NO to NO_2 by oxidation with molecular ozone derived from cylinder air. This reaction causes 10 to 15 percent of the NO_2 molecules to be raised to an excited state and then emit photons. A photodiode detector collects these photons and generates a DC current proportional to the NO contained in the sample gas. This signal is amplified and sent to readouts and outputs. In the NO_X mode, the sensor first uses a NO_X converter to reduce all NO_2 to NO and then repeats the same procedure as above. (Model 400 HCLD Instruction Manual: 23)

A flame ionization detector (FID) determines total Hydrocarbons (THC). This sensor uses a hydrogen/helium burner sustained with carbon free cylinder air. When sample gases pass through the flame, an ionization process produces electrons and positive ions from any hydrocarbons present. A polarized electrode ring then collects the

ions and produces a low current. This current is proportional to the carbon content of the sample gas. The sample is maintained at an elevated temperature for this process. (Heated Hydrocarbon Analyzer Instruction Manual:26)

Mass Flow Measurement

Another fundamental quantity for combustion experimentation is equivalence ratio. This is the ratio of the mass of fuel to the mass of oxidizer in the combustion process. With enough information given it can describe a local region, parts of the combustor, or the entire process. Usually of interest is the variation of emissions products with equivalence ratio. In order to know this value the mass flow rate of both the oxidizer and the fuel must be known.

Thermal mass flow meters measure the flow rate of air into the combustor in the AFIT facility. The device measures airflow by two electronically heated elements. The first element is isolated away from the flow; the second is placed in the air stream. When convective heat transfer with the air cools the exposed element, more energy is sent to the element to maintain the same temperature as the isolated element. This energy difference between the two elements is proportional to the mass flow rate. (Fox Thermal Instruments, Rev. E:1)

Finely controlled syringe pumps control the fuel flow directly. Thus, the user determines the flow rate directly from supplied equipment. Therefore, the fuel flow rate is also a known quantity.

Pressure Transducers and Thermocouples

To establish the thermodynamic state of the air and fuel entering the combustor and for determining losses across the combustor both pressure and temperature are measured at several locations. Pressure is measured by the use of pressure transducers. These devices use deflection of a small diaphragm measured by strain gauges and related to pressure. This signal is amplified and transmitted to an output. Temperature is measured by thermocouples. These consist of two dissimilar metals brazed together at a point. The connection generates a small voltage between the two metals proportional to the temperature of the brazed point.

2.4 Laser Diagnostic Systems

The AFIT combustion facility includes the capability of remote combustion diagnostics using optical techniques. This system uses a double pulsed neodymium-doped yttrium aluminium garnet or Nd:YAG laser with associated equipment to provide six diagnostic techniques useful for combustion phenomena. This includes instantaneous Raman, Particle Image Velocimetry (PIV), Laser Induced Incandescence (LII), Planar Laser-Induced Fluorescence (PLIF), Coherent Anti-Stokes Raman Scattering (CARS) and Raman Spectroscopy. Each one of these techniques provides useful information from the combustor in addition to the data generated from the gas analyzer, thermocouples and pressure transducers.

Instantaneous Raman and Raman Spectroscopy

Instantaneous Raman or spontaneous Raman scattering is a method of scattering laser light off matter to determine its composition. The process is known as instantaneous because the laser energy is returned and collected at a rate faster than the

Kolmogorov characteristic time scale of the flow. Therefore, the measurement is made before the flow field under study has time to change. Most commonly, a single laser in the visible wavelength (400 to 700 nm) is used as a monochromatic source of radiation. Scattering is a momentum interaction between photons. Visible wavelengths are generally used for scattering processes as the strength of the scattered signal scales to the fourth power of the incident wavelength. When this laser light hits matter, Raman, Rayleigh, and Mie scattering occur simultaneously. Rayleigh and Mie scattering consist of elastic exchanges of momentum between photons and different sizes of particles. Rayleigh scattering is when the particle diameter is much less than the wavelength of the incident light, Mie scattering is when larger particles interact with the incident beam. In these cases, there is no change in the frequency of the light as no energy is exchanged with the particles.

Raman scattering is an inelastic scattering of light by the particles of interest. As the term inelastic implies, energy is exchanged with the molecules struck. Depending on the nature of the interaction, the scattering is described as rotational, vibrational, or electronic. Rotational Raman refers to the part of the process where no change in the vibrational quantum number is observed. Otherwise, the process is known as vibrational-rotational or vibrational Raman. Vibrational Raman bands are commonly the most useful for diagnostic use. The returned Raman signal is incoherent, or un-laser like, in nature. The process is often called spontaneous as the interaction is extremely fast compared to other methods, on the order of 10^{-12} seconds or less (Eckbreth, 1988: 12). Due to the exchange of energy between molecule and light, the Raman signal shifts in frequency from the incident source. When energy transfers from the photon to the molecule, the

light shifts to a lower frequency and higher wavelength. This is known as a Stokes shift. If the molecule is in a sufficiently excited state before the interaction, it may lend energy to the photon causing the opposite, or anti-Stokes, shift to a higher frequency and lower wavelength.

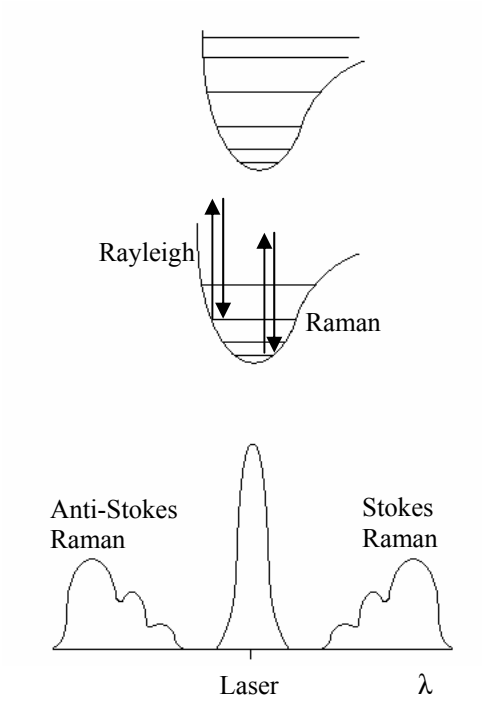

Figure 12: Incoherent light scattering and resulting spectra. The upper diagram indicates two electronic energy states with vibrational energy levels. Upward arrows indicate increasing energy. Raman and Rayleigh scattering are shown. The symbol λ indicates signal wavelength. (Eckbreth, 1988:11)

Due to the quantization of molecular energy states, the Raman spectrum is at fixed frequency separations from the laser line, as shown in Figure 12, and is dependent on the molecular species. Thus, the captured Raman signal is species specific, with the unique signal strength being linearly proportional to the number density of the species. The vibrational frequency seperation of several species of interest are shown in Table 1. The distribution of the Raman spectrum is also characteristic of the temperature, and density measurements can be inferred. Therefore, instantaneous Raman is used for point measurements of species concentration, thermometry and density inside any accessible

part of a combustion device. Like most laser diagnostic techniques, it is considered non-intrusive, although the addition of energy to the flow field of interest by the laser does have a small effect.

Table 1: Fundamental vibrational frequencies of selected molecules of interest. The vibrational frequencies represent the Stokes shift of the incident light for Raman techniques.

Molecule	**Vibrational Frequency (cm^{-1})**	**Molecule**	**Vibrational Frequency (cm^{-1})**
C_2	1854.8	O_2	1580.2
	1641.3		1509.0
	1470.4		1432.7
	1608.2		805.0
	1788.2		700.4
	1809.1	OH	3725.0
	1106.0	radical	3184.3
CH	2858.7	CH_4	2916.5
radical	2930.7		1533.6
	2250		3019.5
CO	2169.8		1306.2
	1743.0	C_2H_2	3372.0
	1515.6		1973.5
N_2	2358.0		3294.8
	1460.6		~611.7
	1735.0		~729.1
	1694.0	CO_2	1388.0
NO	1904.0		667.0
	1903.7		2349.0
	2371.3	H_2O	3657.0
	1036.9		1594.7
			3755.7

Quenching is any one of a number of interactions competing with the desired signal emitting process. These interactions take the form of chemical reaction, dissociation, energy transfer to another molecule, and energy transfer to other states within the same molecule. This is often a serious issue for laser diagnostic techniques as signal strength, and therefore accurate measurement of number density is lost. However, Raman scattering signal strength is unaffected by this process. Instantaneous Raman is also advantageous as a relatively simple and straightforward technique: Only one laser in any wavelength is necessary (although a visible wavelength is usually used), and

collection of the signal does not require through optical access to the region of interest. Calibration requires only the use of nitrogen for comparison. It also has the capability to monitor several species simultaneously, with the same laser. In fact, the same process is used to analyze solids, liquids or gases. In addition, resonant frequency enhancement can increase the signal up to six orders of magnitude if the laser is tuned to be near the resonant frequency of the molecule of interest (Eckbreth, 1988: 13). Spectral interferences between the vibrational Raman bands of different gas types are rare, leading to easy distinction of species. The cleanliness of these Raman spectra is also well suited to thermometry.

However, Raman is generally considered problematic for studying much practical combustion phenomena. This is mostly because the scattered signal is very weak with cross sections around 10^{-31} cm^2/steradian. This results in a collected Raman to laser energy ratio in flames of 10^{-14} (Eckbreth, Bonczyk and Verdieck, 1979: 253). Also, although Raman signals do not attenuate in clean flames, they are affected greatly by particulates. This can result in high uncertainty of measurements as uncertainty is directly linked to flow cleanliness and signal to noise ratios. Thus, in uncontrolled environments, instantaneous Raman is plagued by low signal to interference ratios, making it difficult to use in unclean flames of practical interest. To compensate, relatively high incident beam energy must be used. Also, resonant enhancement can boost signal strength, but for molecules of interest in combustion this is often in exotic frequencies. Thus, it is not possible to perform such signal enhancement on many species with common laser systems.

There are a large variety of experimental setups and techniques based on the concept of Raman scattering. In fact, most of the laser diagnostics for combustion use similar equipment. Historically, typical Raman setups include the use of continuous wave gas lasers such as Ar+. It is also common to use a frequency doubled Nd:YAG laser at a wavelength of 532 nm (green). This laser source passes to reflective mirrors and spherical lenses, typically arranged in what is known as a roof top design, to create multiple passes of the laser. This serves to enhance the Raman signal and make measurements easier to take. Use of a spherical mirror positioned opposite of the collecting device also helps boost signal strength.

Several large lenses focus the signal on a collection device to collect scattered light. Usually this device is a monochromator, used to eliminate certain frequencies of light. This removes the very intense Rayleigh scattering at or near the wavelength of the laser. Bandwidth filters are also used in laser diagnostics to remove unwanted wavelengths. In the case of Raman Spectroscopy a spectrometer is used to diffract the collected light into spectra. Raman spectroscopy involves the study of the spectra resulting from this process. Either a photomultiplier tube or, more commonly in contemporary practice, a charged coupled device (CCD) camera collects light passing from the collection device for analysis. To improve the capture of the Raman signal intensified CCD's are also regularly used.

The use of gating (timing of camera exposure) can help reduce signal interference greatly by cutting out the fluorescent and other more delayed responses of matter to the pulsed laser. To take advantage of gating, a scheme must properly time the camera

exposure within nanoseconds. Commonly the Q-switch in the pulsed laser is the trigger source.

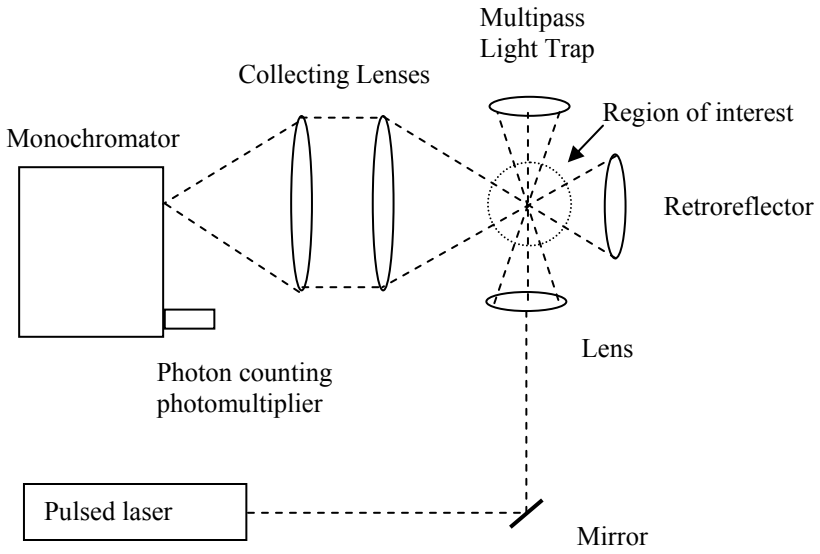

Figure 13: Basic setup for a time averaged Raman measurement. CCD cameras are commonly in use today in place of photomultipliers. (Eckbreth, 1988:190)

CARS

CARS (Coherent Anti-Stokes Raman Scattering) is a complex diagnostic method utilizing Raman shifts and non-linear interactions to produce an easily collected coherent signal. It can be considered similar to instantaneous Raman scattering in result, but is not plagued by low signal strength.

The method involves the use of three or four colors mixing to create a new signal. Specifically, a pump beam with a frequency of ω_1 focuses on a location. A probe beam of frequency ω_2 with a Stokes shift from the pump, matched to the vibrational Raman shift of the molecule of interest, is introduced at the same location. The beams are phase matched to ensure constructive signal growth, and the matching of the mixed signal to the specific molecule of interest provides resonant enhancement. The beams mix to generate a new beam at frequency $\omega_3 = 2\omega_1 - \omega_2$ (where ω is the radial frequency).

The beam mixing occurs through the third order nonlinearity of the electric susceptibility. Susceptibility is the ease of a material's polarization in response to an electric field, such as that created by the propagation of light photons. This susceptibility is dependent on density and temperature of the medium. The nonlinear response of the matter incident to the incoming beams generates an oscillating polarization at the frequency ω_3. The mixing is termed third order because the oscillating polarization is generated in the third order non-linear term of the susceptibility equation. The resulting signal is a coherent radiation containing information useful to the measurement of species concentration (due to the Raman shift), temperature and density with good signal strength. (Eckbreth, 1988:23, 226)

This improvement on signal strength in a coherent form is the major advantage of CARS. The signal is many orders of magnitude greater than Raman scattering at atmospheric pressure is. The coherence of the resulting radiation also improves the signal to interference ratio as the complete signal can be captured in a small angle, therefore limiting the amount of interference. The signal is anti-Stokes shifted, and thus also free from many fluorescent interferences (see Figure 12). Its ease of use exceeds other coherent Raman techniques, and it is the diagnostic of choice for most harsh, practical and dirty combustion environments.

The process is best suited for measurements of major species and thermometry (Eckbreth, 1988:223), and does both simultaneously. It works well with non-reacting flows in temperatures from below ambient to 3000K and pressures from sub-atmospheric to 100 bars. The reported accuracy is often within 2%, and it is successful for both turbulent, time varying applications and steady phenomena (AIAA Reference Sheet).

The universality of the vibrational modes responding to the Raman Effect means the technique is applicable to any molecule requiring obtainable light frequencies. The most common molecule probed is N_2, but other typical species for combustion include H_2O, CO, CO_2, C_2H_2 and CH_4. As with Raman, CARS temperature is determined from the shape of the spectral distribution, and concentration of species is dependent on signal strength. However, uniquely to CARS, the spectral distribution is often concentration sensitive.

There are many disadvantages to this process as well, most of them arising from its complexity: First, the probe beam is specific to only one species, therefore another probe beam must be introduced to obtain good multiple-species data. The coherent signal is directed away from the incident beams, therefore through optical access is necessary. Phase matching is necessary in any three or more color technique, and adds to the technique's complexity. Also, the resulting spectra are very complex relative to instantaneous Raman and sophisticated programs must be employed to analyze the data. Finally, CARS species concentration sensitivity is on the order of instantaneous Raman. This means it is relatively insensitive compared to other techniques. Thus, it is only useful for major species exceeding 0.1% concentration in the probed volume.

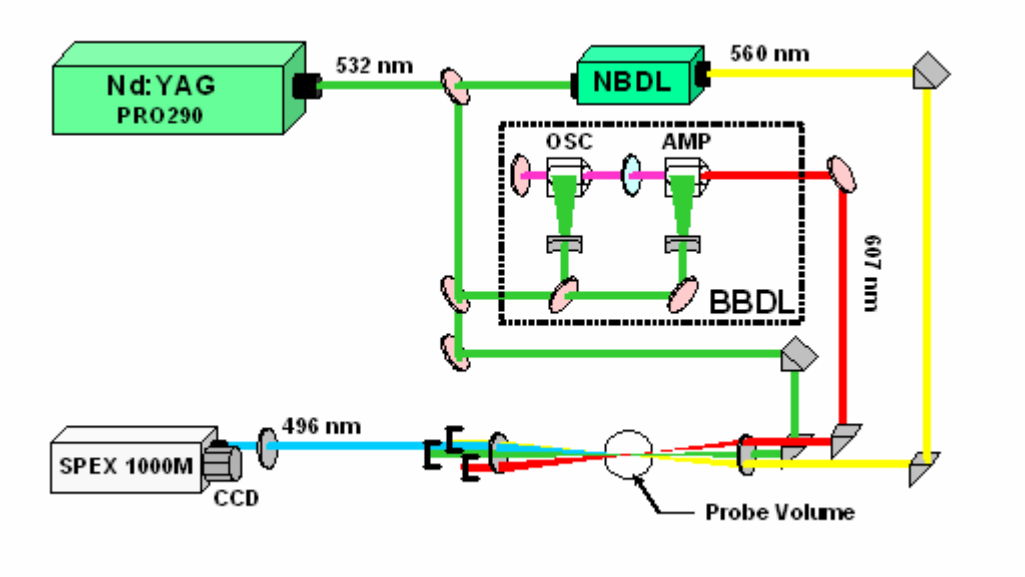

Figure 14: Example of dual-pump CARS experimental setup for N_2-CO_2 measurements. OSC is oscillator, AMP is amplifier, NBDL is a narrowband dye laser, BBDL is a broadband dye laser and the SPEX 1000M is a 1.0m spectrometer. (Roy, Meyer, Lucht, et al, 2005:22, used with permission)

The setup of CARS is much more complex than instantaneous Raman, but it does contain many of the same basic components. Although early CARS studies utilized ruby lasers, it is now more common to see frequency doubled, pulsed Nd:YAG lasers implemented. This laser is usually split into two or more beams at 532 nm. One or two of the beams pump the Stokes dye laser(s), usually at 550 to 700 nm depending on the molecule of interest (Eckbreth, 1988:247). The remaining pump beam focuses with the Stokes beam on the point of interest through a lens. An opposing lens then re-collimates the light. The coherent signal passes to a spectrometer, and subsequently to an intensified CCD camera. Gating enhances the results.

PLIF

Planar Laser Induced Fluorescence is a two dimensional diagnostic technique taking advantage of the absorption and emission of photons. Fluorescence is the emission of light from an atom or molecule after it is moved to an excited state by

various means. In the case of laser diagnostics, photon absorption is the preferred means of excitation. Simply put, in fluorescence the atom or molecule absorbs an incident photon, this in turn forces the electrons in upper levels to higher energy states, as shown in Figure 12. In an effort to return to an equilibrium electron configuration, the atom or molecule releases another photon at a different wavelength. Fluorescence is the term for the specific case where emission occurs between electronic energy states of the same multiplicity, or spin. This is opposed to phosphorescence, where emission occurs between states of opposite spin. Fluorescent lifetimes are several orders of magnitude longer than Raman scattering, varying between 10^{-10} and 10^{-5} seconds (Eckbreth, 1988:14). As shown in Figure 15 emitted light may be at a Stokes shifted frequency or it may be at a resonant fluorescent frequency matching the incident beam. Usually, the shifted frequency is utilized for measurements, as it reduces interferences with particle scattering.

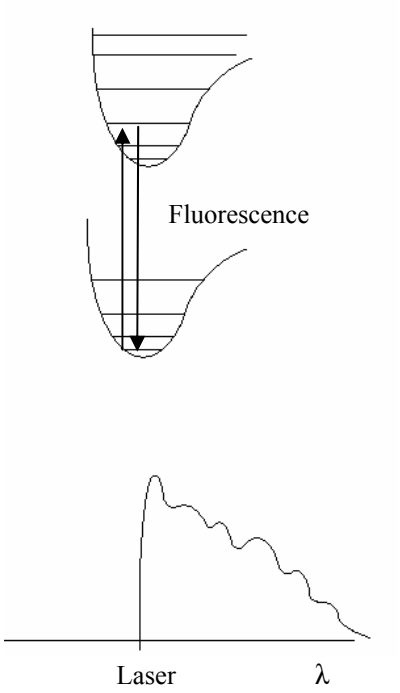

Figure 15: Fluorescent absorption, emission and resulting spectra. The upper diagram indicates two electronic energy states with vibrational energy levels. Upward arrows indicate increasing energy. The symbol λ indicates signal wavelength. (Eckbreth, 1988:11)

As with Raman scattering, the resultant signal occurs in all directions and is incoherent. Also as with Raman, the quantization of molecular and atomic energy states results in discrete regions of spectral absorption. This means fluorescence is species specific. The intensity of the signal is a generally linear function of number density of a given species and is a function of temperature and pressure.

Unlike Raman scattering, the use of fluorescent techniques requires consideration of quenching. Quenching has a large affect on the strength of the signal emitted, and its variability can make data very uncertain. If detailed quenching data and the concentration of quenching species is known, then analytical models can be used to adjust for quenching affects. However, this is rarely the case. Thus, fluorescent

techniques often involve partial or complete saturation of the medium under study. This eliminates quenching issues by permitting corrections to be determined in-situ.

PLIF takes advantage of fluorescence in a particularly useful way. Using cylindrical optics the laser source is projected as a sheet into the region of interest. The beam is usually pulsed and tunable to a wavelength resonant with the optical transition of the species of interest. Because of this resonance, a fraction of the light will be absorbed at each point the species resides within the laser sheet, another fraction of these photons emit in fluorescence at the shifted wavelengths. A solid-state array camera collects the light. The intensity of the fluorescence in the volume relates to the amount of light captured by the camera at a corresponding location. Thus, the concentration of a particular species, temperature, and pressure is measured. Utilizing the Doppler shift of the signal, velocity measurements can be taken.

Flow fields are often measured using PLIF by seeding with an appropriate substance that will fluoresce. In the case of combustion diagnostics, this is usually unnecessary as concentrations of good fluorescing compounds such as Na, OH, NO, O_2, CH, CO and acetone are already present. OH is an important and plentiful radical in combustion sequences, and is therefore often used as a flame locator. NO is often imaged to determine locations of NO_X production.

Table 2: Major allowed electronic transitions for species of interest. These transitions represent the bands active to fluorescent absorption. (Eckbreth, 1979:260-265)

Molecule	Electronic Transition (nm)
C_2	400-600 230-330
CH radical	500-430 450-360
CO	200-250 150-240
N_2	100-500 Vac u.v.
NO	195-340 200-500
O_2	500-900 170-220
OH radical	240-400
CH_4	145.5-500
C_2H_2	237-210
CO_2	140-170
H_2O	145-186

As Table 2 shows, the range of the major electronic transitions for absorption cover a wide band and are usually centered about the ultra-violet region for combustion molecules. However, only certain discrete wavelengths in these regions are actually allowed by the rules of quantum mechanics. In addition, it is desirable to discover the transition wavelength with the highest absorption to produce maximum emission. Because of the complexity of these rules, computer software is often used to determine the appropriate wavelengths for excitation and collection. Examples of spectra developed by the software package LIFBASE is shown in Figure 16 (LIFBASE website).

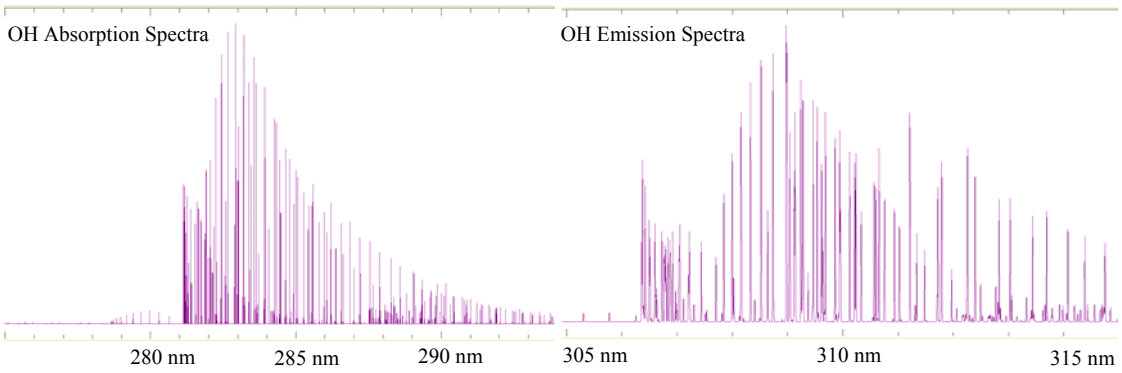

Figure 16: Fluorescent absorption and emission spectra for the OH radical at 2000K and 1 atm in air. These plots were produced with the LIFBASE software. They show maximum absorption at nearly 283 nm and maximum emission at 309 nm.

Fluorescence offers many advantages over other techniques: its signal strength is many orders of magnitude larger than even near-resonant Raman scattering. This enables it to be used in a PLIF sheet and still detect minor species on the ppm level. Also, fluorescent absorption of molecules such as CO_2, CO, H_2O and C_2 reside in ultraviolet and visible ranges (200 to 600 nm) that are accessible by common equipment.

There are also many disadvantages to the use of fluorescence and PLIF. Due to the large affect of quenching and limited data on quenching mechanisms, this technique can be problematic. In order to identify species, an emission spectrum for the molecule must be known. However, due to quenching difficulties this information may not be available for many species. Also, the rate of radioactive decay of the excited state must be a known quantity as the fluorescent power is proportional to this rate. The shot-noise of the detector often limits the signal to noise ratio of PLIF. Fluorescent interference from un-probed species is also common, especially those from hydrocarbons when reacting under high pressure. Interference from infrared emissions of stable molecules is an issue. The PLIF laser sheet can often attenuate significantly across the flow field. Some species of interest prove difficult to study, as they do not have excitation

frequencies commonly available from a single source. In fact, temperature measurements usually require two laser sources and homonuclear radicals such as C_2 cannot be detected (AIAA Reference sheet). Research has shown that velocity measurements are usually only practical for high Mach number flows. Fluorescence runs a higher risk of laser-induced chemistry, although this is normally avoided with the use of faster (nanosecond) pulsed lasers (Eckbreth, 1988:305). Finally, the use of laser sheets usually requires optical access at perpendicular orientations to capture results.

The general setup of PLIF is similar to the other laser techniques. Again a pulsed, frequency doubled Nd:YAG laser is commonly used to pump a dye laser. The resultant beam usually passes through a frequency conversion assembly in order to produce the required frequency for fluorescence of the molecule of interest. In PLIF a cylindrical lens then creates a laser sheet photographed by a high resolution or intensified CCD camera in a position approximately perpendicular to the sheet. The camera is gated and timed, usually off the Q-switch of the source laser.

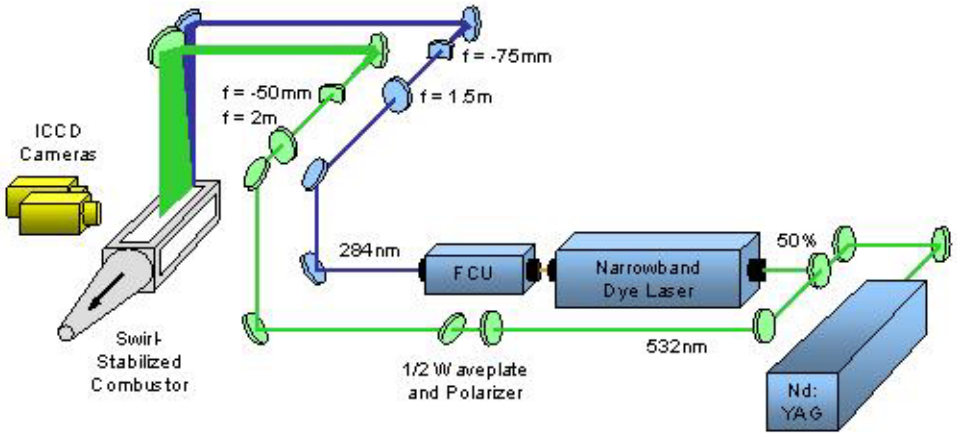

Figure 17: Schematic of experimental setup for conducting simultaneous LII and OH PLIF measurements. The OH PLIF is provided by the pumped dye laser at 284 nm. (Meyer and Roy, 26:2003, used with permission)

LII

Laser Induced-Incandescence (LII) uses the release of blackbody radiation to track particulates in a flow field. Incandescence is the release of electromagnetic radiation from a hot body at a high temperature, such as a filament in a light bulb. Photons emit when electrons jump to higher states due to the energy absorbed by the heating process. This phenomena occurs for all matter, but is usually in the infrared spectrum, and thus invisible to the naked eye below 900K. The intensity of emission increases with temperature, with the peak signal wavelength shifting towards smaller wavelengths (blue) according to the Planck radiation law.

For combustion diagnostics, this technique is of use for determining the volume fraction of soot in the flow. If a laser of sufficient energy is used, the pulsed light can heat soot particles of typical size (20 to 50 nm) so they incandesce in a blue shifted frequency, even inside the flame. This blue light is detected easily when captured before cooling occurs within nanoseconds of the laser pulse (Vander Wal, 1997:1). Theory predicts the intensity of this incandescence correlates to soot volume fraction. This is because the soot particles are much smaller than the laser excitation wavelength, and thus can be considered volume absorbers. However, in reality the soot is not a perfect volume absorber. Thus, calibration is used to determine the exact volume fraction (Wainner, 1997:2), with uncertainties of the order of 10% (AIAA Reference Sheet). This process has also been used in a limited manner to determine the size of soot agglomerates.

LII has multiple advantages. It is well suited for both steady and rapidly changing phenomena as observations can be made from a single laser pulse. This is usually every 10 ns (Vander Wal, 1997:1). Spatial resolution is also good. The process is nearly

independent of scattering by aggregates and absorption of polycyclic aromatic hydrocarbons (PAH's), molecular fluorescence or flame luminance. The technique requires no through optical access. Planar measurements are possible and commonly used with the creation of a laser sheet.

The major disadvantages include the requirement of calibration. Measurement uncertainty increases with deviation of actual conditions from temperature and soot agglomerate size used in calibration. Although most fluorescence is not an issue, some types can interfere with the LII signal. Also, inconsistent particle heating can be problematic. Like PLIF, high particulate concentrations and long beam path lengths can cause attenuation of incident beam or LII signal across the measurement volume. This introduces errors to the readings. The process also requires use of a higher intensity laser, at least 50 to 100MW/cm^2. Fast gating detectors are also necessary (less than 50 ns for lasers with 5-10 ns pulse durations).

LII setup uses similar equipment to the other techniques discussed. In this case it is not uncommon to use a pulsed Nd:YAG laser at its normal frequency of 1064 nm (infrared) although other sources are also used at 532 nm. The most important aspect is the beam must have sufficient power to heat the soot particles quickly. From this beam a laser sheet, as seen in Figure 17 or small investigation volume is made using an appropriate lens. Bandpass filters block light outside of the blue wavelengths of interest for collection. A CCD camera or monochromator with photomultiplier tube capture the LII signal. Like all other techniques, gating improves the signal reading.

PIV

Particle Image Velocimetry (PIV) is another two-dimensional technique that seeds the flow field with particles and directs a laser sheet across a region of interest. The particles are often injected in gaseous or liquid form, and usually consist of visibly reflective material. Pulsed laser light and a properly timed camera (either film or CCD) take successive pictures of the particles as they travel through the laser sheet. The location of the particles in the flow can be determined using the geometry of the setup and location in the picture. A variety of approaches, most statistically based, then match the same particle from one frame to another. Using this information, a simple first-order differencing between two successive frames gives an average velocity of the particles. If the experiment is set up correctly, this velocity very nearly approximates the flow field of interest.

There are several categories of similar techniques grouped under the heading of Pulsed Light Velocimetry (PLV). PIV itself can be distinguished by the use of high image density (HID) or low image density (LID) techniques. Larger numbers of particles are seeded in the flow in the high-density case. Here a correlation is generally used to track particle motion. However, in LID individual particles can be picked out. Laser Speckle Velocimetry (LSV) is a method using extremely dense seeding and study of the resulting speckle patterns. However, due to the high density necessary, this technique is seldom used, and a smaller number of molecular or particulate markers are usually employed (Benard and Wallace, 2002:165). In fact, PLIF can be used as another form of PIV, where fluorescing molecules replace optically reflective particles. However for

most flow phenomena investigated by PIV, particles such as atomized olive oil are used to seed the flow.

Care must be taken to balance the particle size and light sheet thickness between conflicting requirements. The particles must be small enough to correctly follow the flow field, but large enough to effectively reflect the laser light. The laser sheet must be thick enough to capture a significant number of particles in each frame, but not so thick the particle's velocity would be out of the plane of the sheet. Also, the out-of-plane component of velocity must be accounted for in many cases for the sake of accuracy. To determine direction of the particles image shifting, where the second image taken by the camera is shifted slightly, must be used.

PIV has the advantage of using a single laser to create a two-dimensional measurement using a cylindrical lens. The laser is usually in the visible spectrum and a camera with sufficient gating capability is all that is necessary to collect data. The method is the best means of experimentally mapping a velocity flow field.

PIV's major disadvantage is the necessity to seed the flow. Seeding the flow can be messy, and sometimes impractical. The substances necessary to seed combustion flows are often hazardous as well. Also, in the combustion environment background luminosity, soot particles or other phenomena can interfere with the reflection off of seeded particles. In addition, some knowledge of the flow must be had before experiments can be run, as the laser should be pulsed at a characteristic time to capture the complete motion in the flow field. Velocity is the only data available from the use of PIV, and only low speed flows can be mapped.

PIV setup requires some differing equipment than other combustion techniques. The diagnostic uses light at visible wavelengths such as 532 nm or 355nm. These may be created by a Nd:YAG signal that is mixed using harmonic crystals. If the beam is not pulsed, a shutter mechanism may be used. Also, the laser beam is often passed onto a mechanical device to provide image shifting by timed rotation of mirrors so velocity direction can be assessed. From here, a lens creates a laser sheet across the flow of interest and a film or CCD camera is used to take pictures of the flow in rapid succession. Timing is important in PIV as well, but more so for temporal resolution of the photos to determine the flow field than improving signal collection. An appropriately designed flow seeder is also necessary in PIV.

III. Methodology

3.1 System Design and Operation

The laboratory is located in room 258 of building 640 at the Air Force Institute of Technology. It is designed to facilitate small-scale combustion experimentation at atmospheric pressure. The facility features five central elements: First, a computer control station provides remote operation and data collection for experiments (seen in Figure 18). Secondly, a laser diagnostic system enables advanced data collection such as PIV and PLIF. Third, various operation and measurement systems throughout the room give basic functionality to the lab. Fourth, a combustor stand gives a place to physically mount the combustor, and support equipment. Finally, a Unistrut cage, 20 feet by 10 feet, encloses the experimental area, and provides support for wires, tubes and cables. This clears the floor of clutter and enables the easy location of the laser diagnostic system.

Figure 18: California Analytical Instruments raw exhaust analyzer test bench (l) and laboratory computer control station (r).

Computer Control and Data Acquisition

Almost all of the laboratories major systems are integrated through the main control station. From here, the individual conducting the experiment can operate all the major equipment, record data, and initiate an emergency shutdown if necessary. Several pieces of National Instruments (NI) Data Acquisition (DAQ) equipment are used for integrating the pieces of the facility with a PC. A LabView VI (Virtual Instrument) provides user interface to the PC and DAQ equipment. Figure 19 contains a wiring diagram showing the general connectivity of the control and measurement systems.

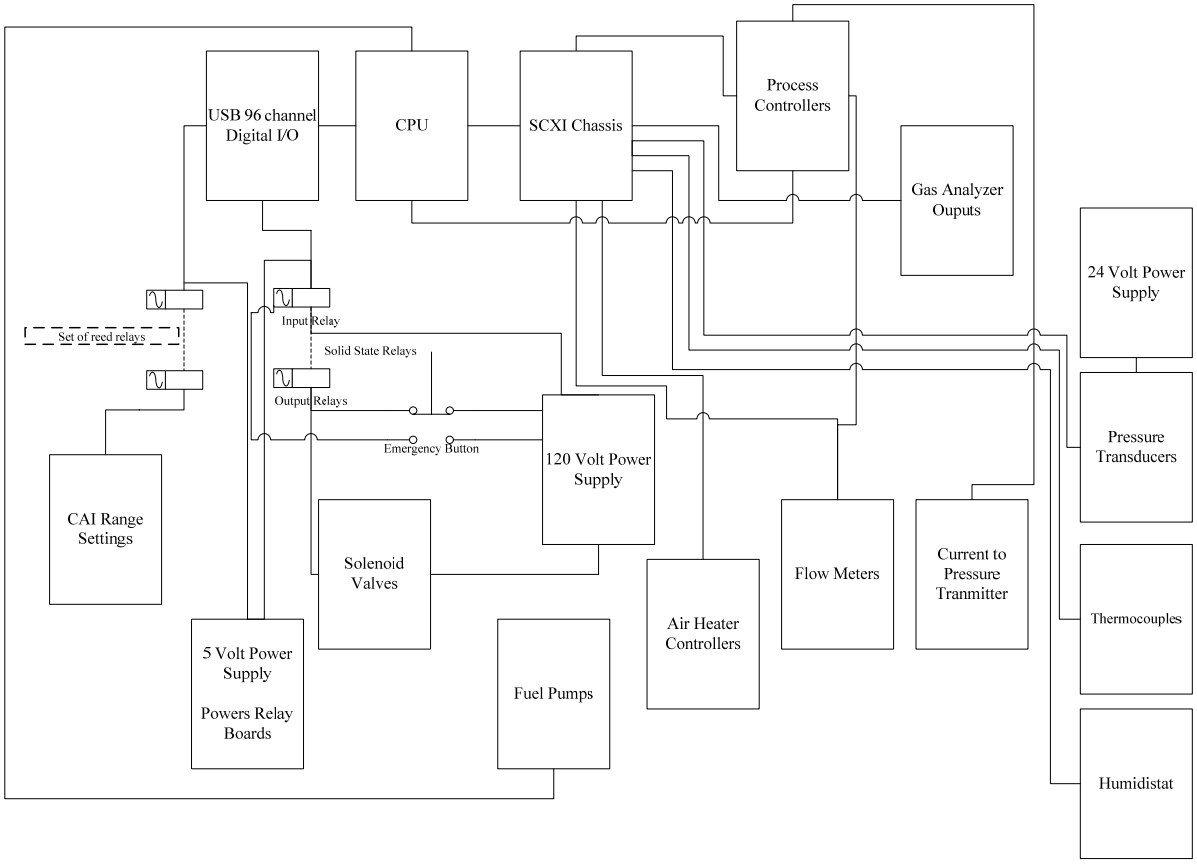

Figure 19: Diagram of control systems connectivity.

An HP dx5150 MT PC operating with Windows XP and installed with LabView 8.2 is the brain of the laboratory. It is located in an electrical enclosure containing most of the electronics hardware. Two devices connect the PC to the laboratory through USB. The first is a National Instruments (NI) SCXI-1600 USB 16-Bit digitizer module. This unit mounts in and provides control of the NI SCXI 1100 Data Acquisition (DAQ) chassis. The chassis acts as an interface with many interchangeable hardware modules. The modules in turn are interchangeable with a limited number of terminal blocks. These terminal blocks connect directly to the equipment throughout the laboratory through signal or thermocouple lines. Most of the information sent by the laboratories measurement equipment are received by the terminal blocks with 4-20mA signals. Control of rig air heaters and the flow control loop is acomplished via 0-5 VDC output signals. Figure 20 shows a detail of the chassis setup. Appendix A details all of the nearly 100 electronic signal connections in the laboratory running through the SCXI 1100 chassis. For ease of installation and modification, spring release wire connecting terminal blocks mounted in the enclosure provide a break in each signal line between the NI terminal blocks and laboratory equipment.

The second device connecting the PC to the laboratory is a NI DAQPad 6508. This device provides digital I/O capability controling two Opto 22 Solid State Relay (SSR) boards. A diagram of the connection of this hardware is shown in Figure 20. These boards act as computer controlled on-off switches for equipment throughout the lab. The first of these boards, the PB24, controls all solenoid valves and the ignition transformer. It also reads inputs from a pressure switch in the exhaust ducts (to ensure the exhaust is operating) and the emergency-shutdown switch (to inform the computer

when emergency shutdown is engaged). This board employs a variety of interchangeable input and output relays. The second board, the G4PB24, is dedicated to remotely operating the range selectors of the gas analyzer system. This board employs 24 optically isolated reed relays. By closing the corresponding circuit, the desired measurement output range is selected on the analyzer. Complete lists of the connections through the DAQPad system are given in Appendix A.

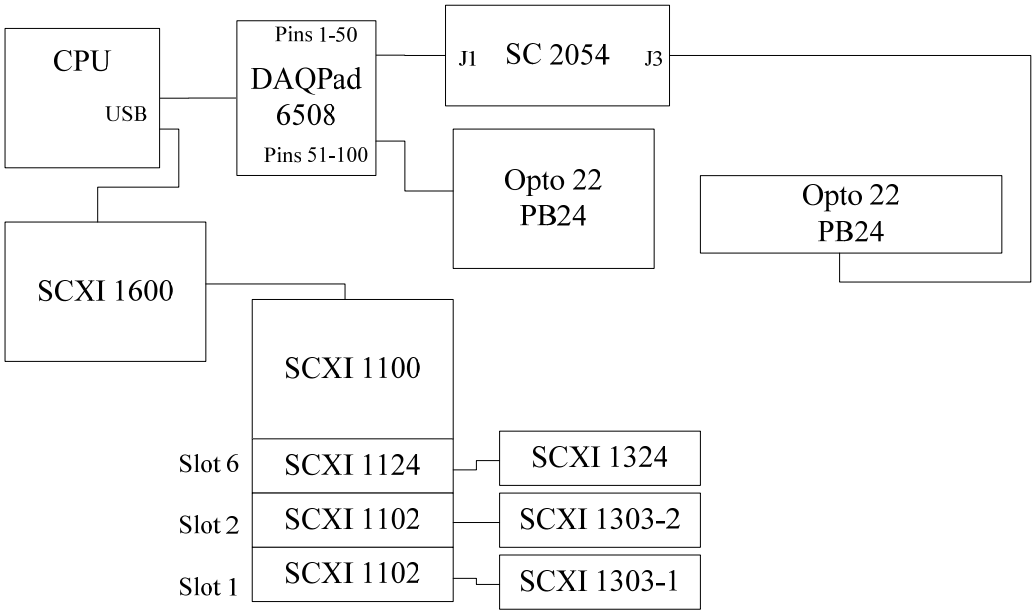

Figure 20: Peripheral hardware what provides direct control of the laboratory systems by the CPU.

Data Acquisition and Control Software

LabView data acquisition software provides the interface between the individual running the experiment through the control station and the hardware controlling the equipment around the laboratory. The LabView software uses a series of VI's connected by wires in the program as if they were pieces of physical laboratory equipment. The overall program is one large VI drawing, built from a library of basic ones. This visual

programming allows the code to be quickly understood by a new user who may want to modify the program. When the main LabView VI is running, a front panel is displayed on the computer's screen. Much like a real instrument, the VI's front panel consists of buttons, switches and displays the user can interact with while the program is operating. Dittman developed the code's organizing structure and most of the programming. However, much troubleshooting, adaptation to systems, connectivity, and modification for usability was completed in the author's work.

Through use of this software, the user can control all systems connected to the computer and automatically record pressure, temperature and emissions data for later analysis. Thus, the LabView VI makes the laboratory easily manageable. A flow chart demonstrating the operation of the software is shown in Figure 21.

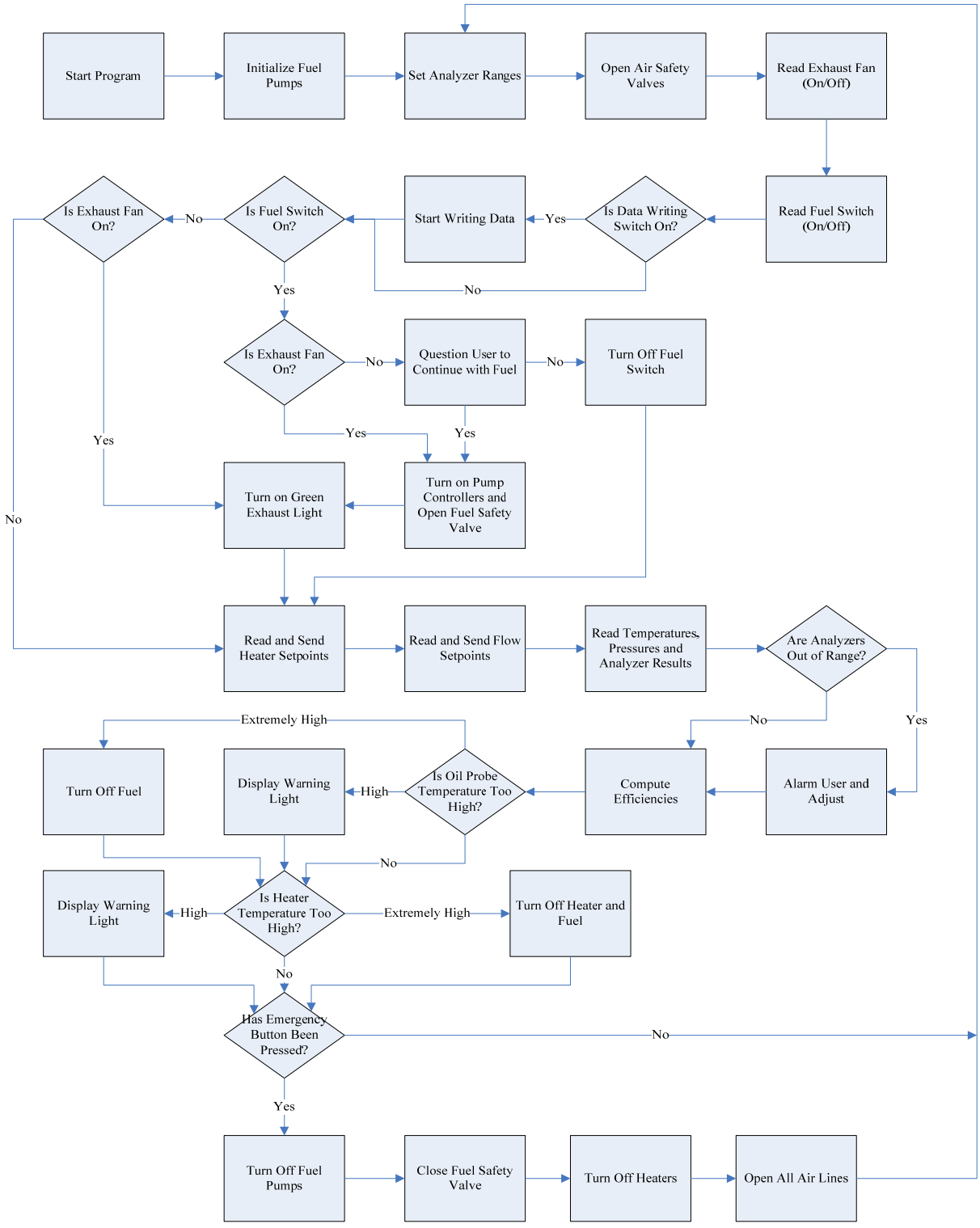

Figure 21: Combustion facility control software flow of operation. (Dittman, 2006:32)

Power supply systems

Power for most laboratory equipment is routed through the control station. Most devices operate on a standard 120VAC/60Hz supply. However, both 5 and 24VDC are provided from the enclosure for varied equipment. The distribution of this power is provided by several terminal blocks, mounted in the electrical enclosure. Figure 22 shows the wiring of both AC power, Figure 23 shows DC. A complex series of signal connections also provides power for the various pressure transducers located in two boxes in the lab, this can be seen in Figure 24.

All AC power used to control valves supplying the combustor system is wired directly through an emergency shutoff button. This is located on the enclosure at the operator's station. The direct connection ensures no hang-ups in the event of an emergency. All systems have been designed for a flameout emergency shutdown. The switch is also wired through the 24 VDC power supply and one of the input relays on the PB24 so the computer can sense an emergency shutdown.

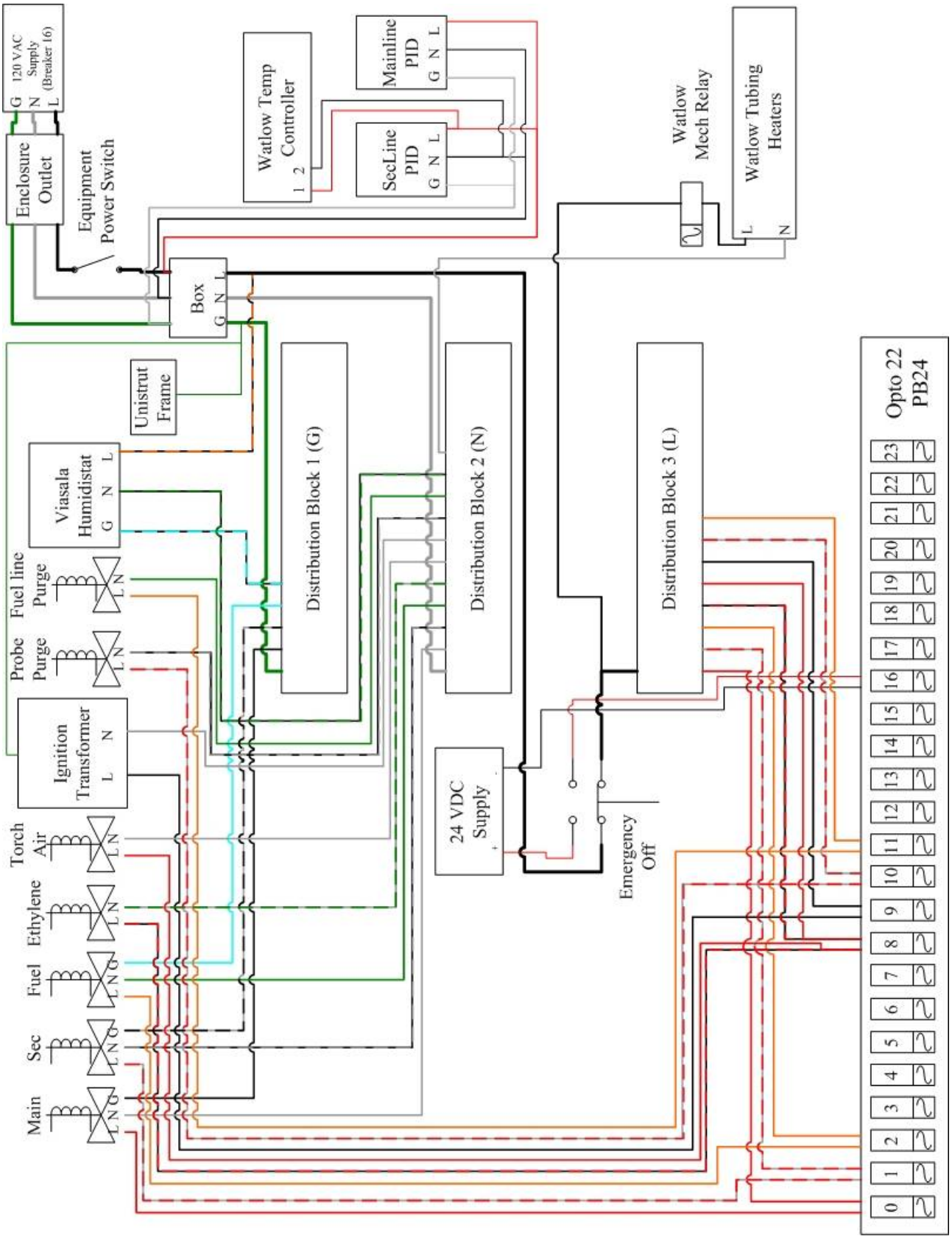

Figure 22: AC Power wiring diagram.

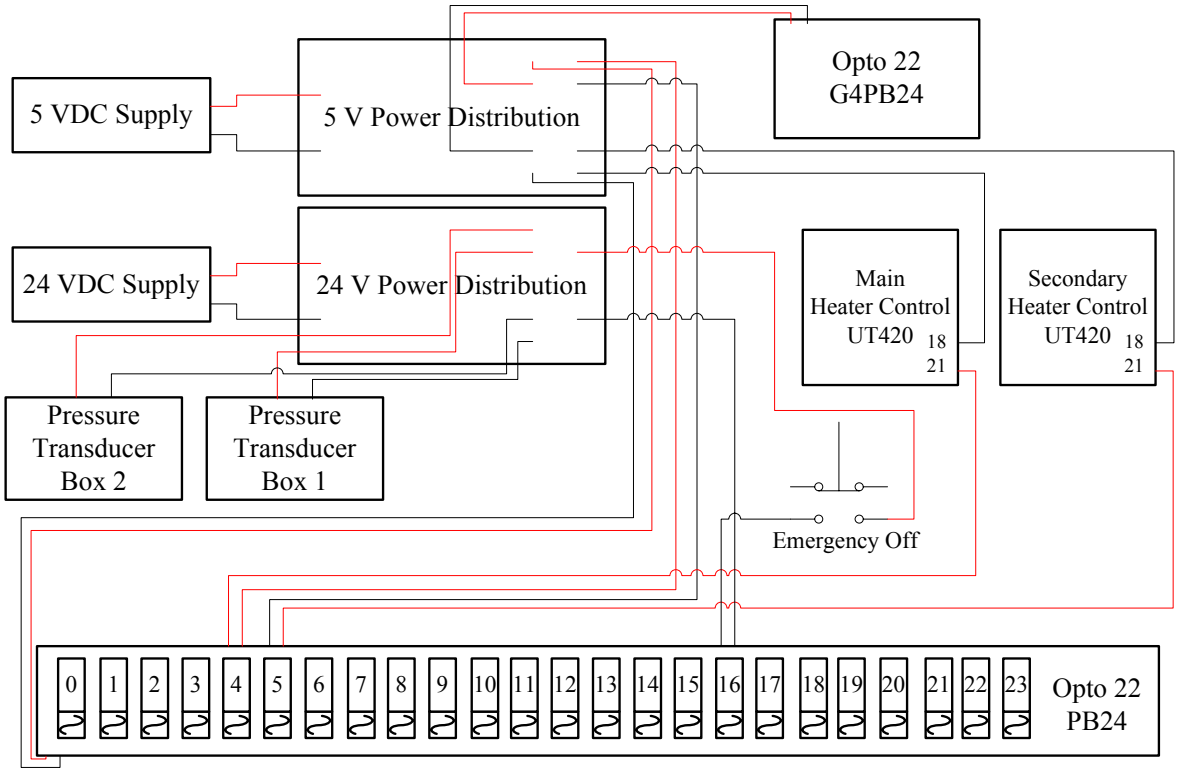

Figure 23: DC power wiring diagram.

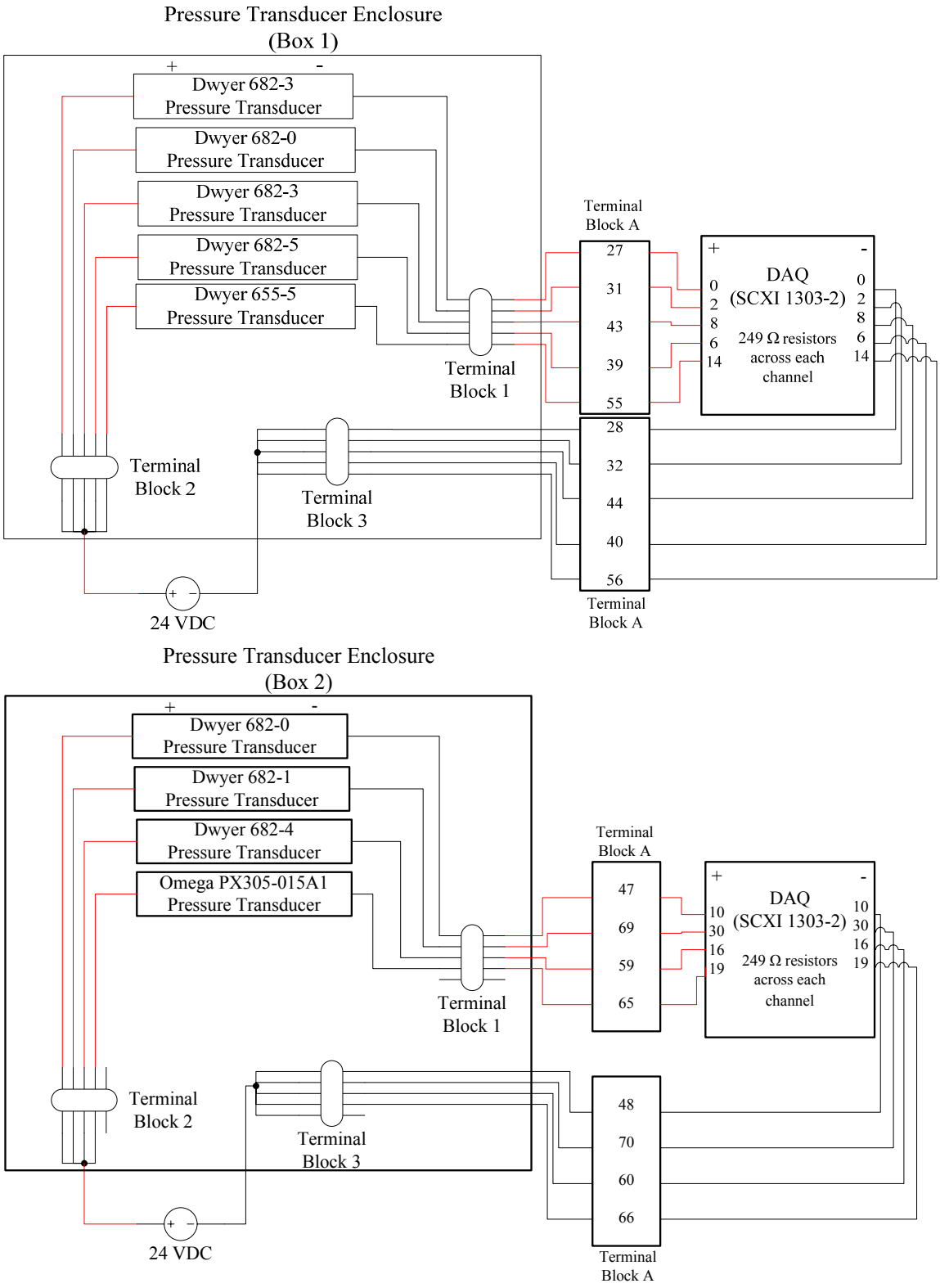

Figure 24: Power distribution and signal lines in pressure transducer boxes.

Combustor Rig Air

Two large airlines provide the combustor rig with a heated air supply (referred to as the rig air) of up to 0.15 kg/s (260 SCFM). The main airline consists of 1.5" pipe used for the majority of the flow (up to 0.12 kg/s or 200 SCFM). The secondary line consists of ¾" pipe for up to 0.03 kg/s (60 SCFM). Two Ingersoll-Rand compressors located in Building 644 provide the rig air at approximately 10.3 bar (150 psig). Air enters the room from the compressor through a single 1.5" copper pipe. The air is then divided into the main and secondary lines. At this point a Viasala DRYCAP Dewpont and Temperature Transmitter measure the relative humidity of the air.

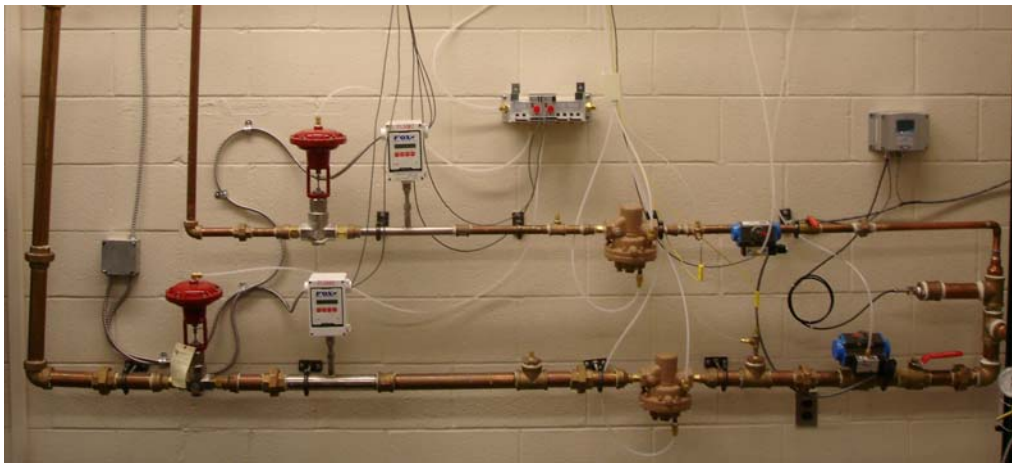

Figure 25: Rig airlines upstream of electric heaters.

Though the lines support different flow rates, they are actually two identical, parallel systems from the point of division to the combustor. For each line, the high-pressure air meets first a manual and then a UCI pneumatically actuated ball valve. An electronic solenoid valve mounted on its body in turn operates the pneumatic valve. This solenoid valve and all others in the system turn on and off through use of the Opto 22 PB24 SSR board, operated by the computer at the control station. Pressure and temperature of the air are measured just downstream of the pneumatic valve by a Dwyer

682-0 pressure transducer and a K-type thermocouple. The air pressure is then reduced by a CASHCO pressure-reducing valve (PRV) controlled by manual manipulation of a pressure regulator located at the control station. This pressure difference is what drives the flow and provides rough control of the rig airflow rates. The delivery of the maximum flowrates provides enough air to achieve proper cavity velocities in the UCC as based on the work of Quaale. (Dittman, 2006: 18)

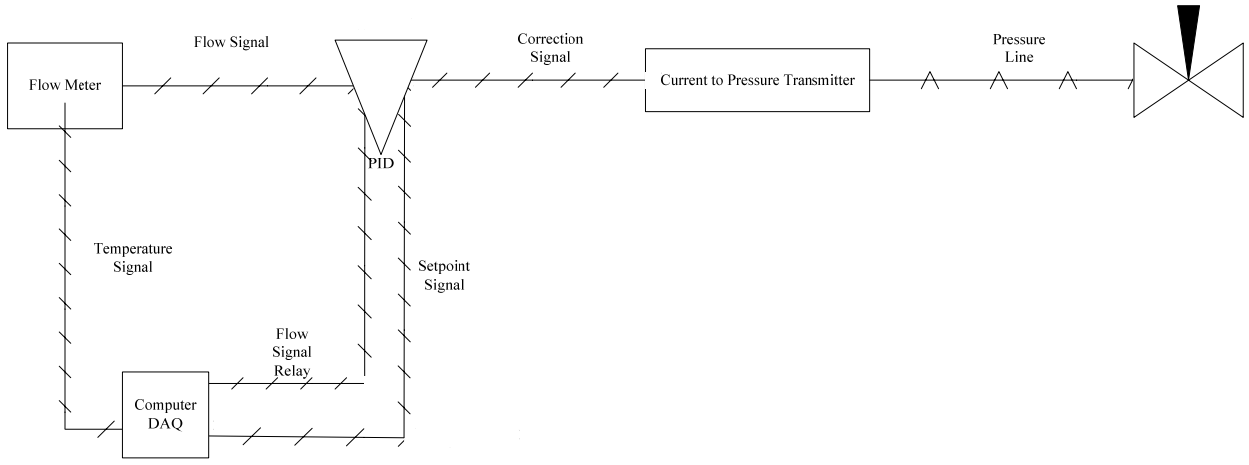

Figure 26: Rig airflow control loop.

Downstream of the PRV a Fox Instruments FT2 thermal mass flow meter measures both the temperature and the flow rate of the air and transmits this information to the control station. After the mass flow meter a Badger Meter pneumatically actuated needle valve provides fine control of the air flow rate. This needle valve is operated from the control station via a Moore Industries IPT^2 current-to-pressure transmitter. Thus, the information from the mass flow meter is used in a control loop with the needle valve to automatically maintain a user specified flow rate. A conceptual drawing of this control loop can be seen in Figure 26, while a detailed signal connection diagram is shown in Figure 27.

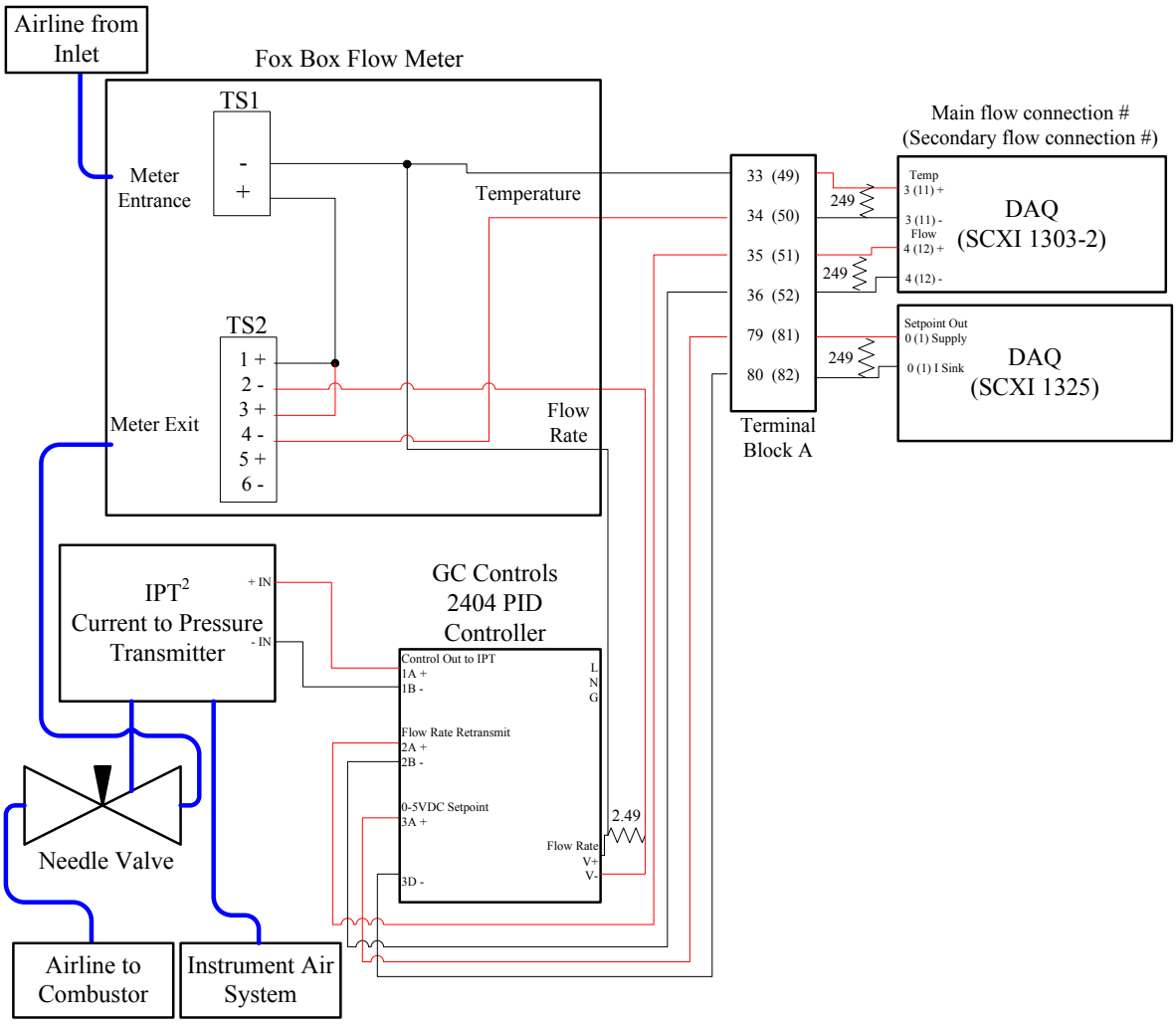

Figure 27: Signal line connection schematic of rig air control loop and data transmission.

In this control loop, the mass flow rate is transmitted to a GC Controls 2404 PID controller mounted at the control station. The PID in turn retransmits this information to the computer for use in data recording and easy user monitoring. After closing in on the desired flow rate with adjustment of the PRV regulator the user can specify the desired flow rate exactly in the LabView VI. This set point information is transmitted to the PID through the NI SCXI 1325 Low Voltage terminal block. The PID then uses proportional-integral-derivative logic to achieve the set point by sending a correction signal to the

current-to-pressure transmitter. This in turn controls the needle valve. By constantly updating this process, the flow rate of each rig airline is maintained.

At this point, the air is nearly atmospheric in pressure and is traveling at the desired mass flow rate. It then enters a Gaumer electric air heater. This device can raise the air temperature up to 810K (1000 °F). However, the flexible tubing connection to the combustor can only tolerate 530K (500°F) and the Teflon pipe dope used to seal the airlines can only withstand 670K (750°F). This heating simulates air exiting a compressor. The heater receives a temperature set point from the control station through the NI SCXI 1325 module and contains its own PID, internally adjusting the heater temperature. This temperature is retransmitted to the computer for data recording. As seen in Figure 28, an emergency shutoff for the heaters is also operated at the control station through the PB24 SSR board. Once the rig air passes through the heaters it feeds through insulated stainless steel lines directly to the combustor for use. At the end of these lines, two high temperature hoses provide flexibility for connection.

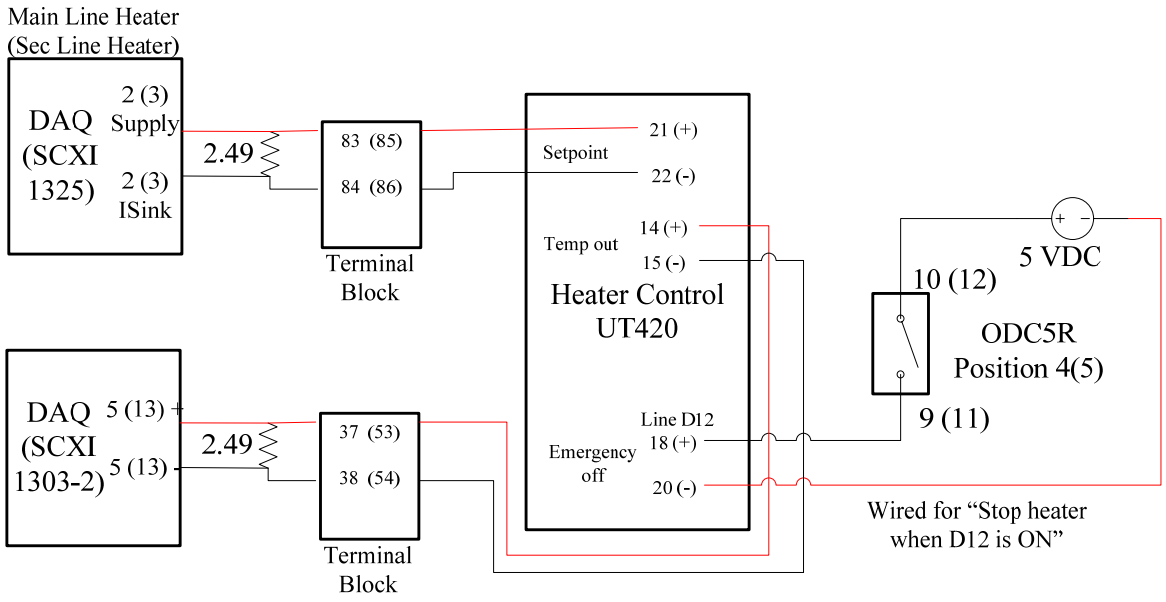

Figure 28: Heater emergency shutoff and data transmission.

Fuel Supply

At this time, the combustion facility is designed primarily to provide liquid fuel (JP-8) operation using two ISCO 1000D syringe pumps. This system uses both syringe pumps to provide fuel at a continuous rate to the combustor. Thus, while one pump is providing fuel, the other is refilling. A pneumatically actuated switching system controls the interchange between the two pumps. The original design requirement was for the creation of equivalence ratios in the combustor similar to past experiments, 0.5 to 4. This meant 4.69 mL of JP-8 per second must be pumped. The ISCO 1000D pump can provide 5.67 mL/s at 137.9 bar with an accuracy of 25.38 nL. (Dittman, 2006: 21) Fuel is provided through a 1/4" stainless steel line able to withstand several hundred bar.

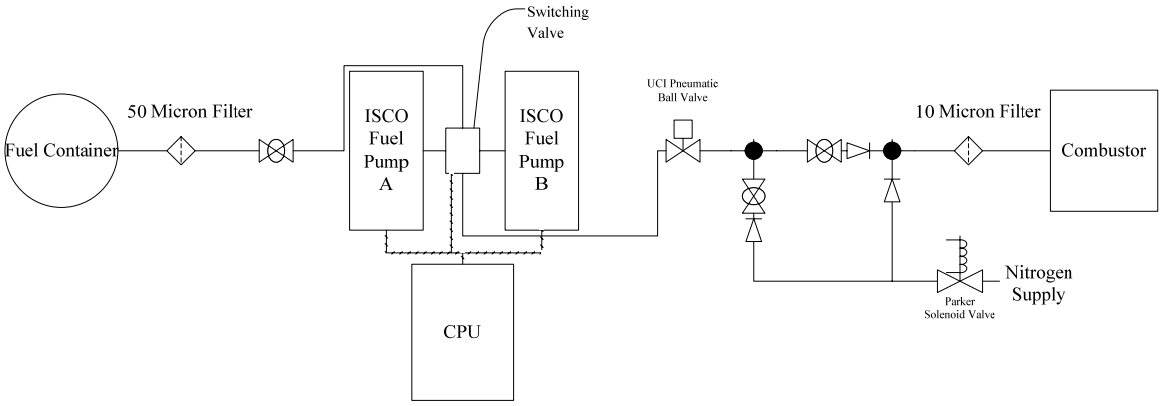

Figure 29: Liquid fuel pump and control system

As shown in Figure 29, the pumps are controlled through a serial connection directly to the PC and the LabView software interface. This LabView pump control program was provided by ISCO and integrated into the laboratory control VI. In addition, another UCI pneumatic valve controlled by an offset Hoerbiger solenoid valve is connected downstream of the fuel pump. The SSR PB24 board operates this too. This UCI valve acts as the emergency shutoff valve for the fuel system. Manual valves located just upstream of the fuel pump, downstream of the pneumatic ball valve and near the combustor stand provide control for fuel line disconnect, purging and emergency shut-off. A pressure tap runs to a Dwyer 682-4 pressure transmitter, and another K-type thermocouple measures the temperature of the fuel line. Thus, the state of the fuel at combustor entry is known.

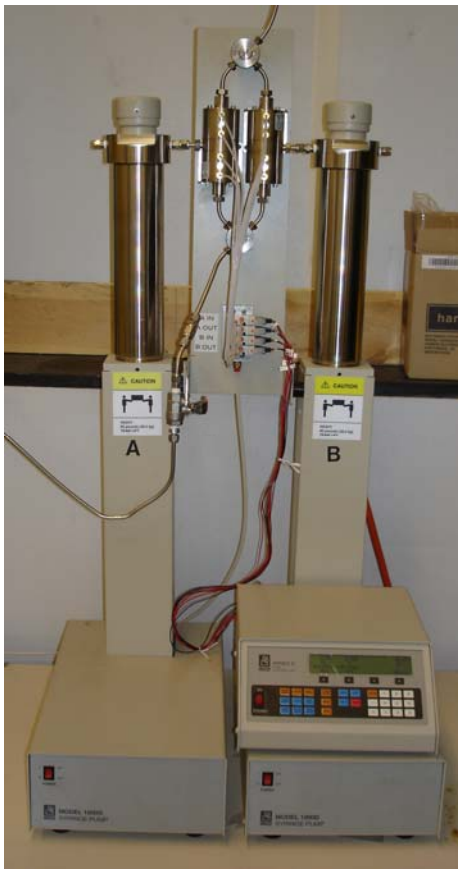

Figure 30: ISCO fuel pump system.

Remote Ignition

For remote ignition of the combustor, an ethylene/air torch was built to attach to one of the combustor sidewalls. Fuel is deposited in this region, and experience with similar laboratory environments suggests this is the ideal location for ignition. Air and ethylene gas are stored in bottles in the bottle farm outside the building and piped in at 30-40 psig. To simplify system operation and reduce control problems from loss of instrument air, bottled cylinder zero air is used as the oxidizer.

Both zero air and ethylene fuel are turned on and off by use of Parker solenoid valves (again controlled by the SSR board). For safety, the ethylene solenoid valve is explosion proof and placed above other nearby valves and electronics (ethylene is lighter than air at room conditions). The equivalence ratio of the torch must by preset by two

metering valves located before the mixing point on the combustor stand. Check valves prevent propagation of burning gases from the combustor into the supply lines. An AC Delco R44LTSM automotive spark plug ignites the torch at the combustor. Electricity is run through metallic, single conductor spark plug wire to provide remote ignition. A Dongan A10-LA2 ignition transformer also wired through the SSR PB24 control board provides sparking power. Grounding is provided through the combustor stand, and is connected to the Unistrut laboratory frame. This in turn is earth grounded through the electrical system. This grounding is common to the ignition transformer, as is necessary for its proper operation.

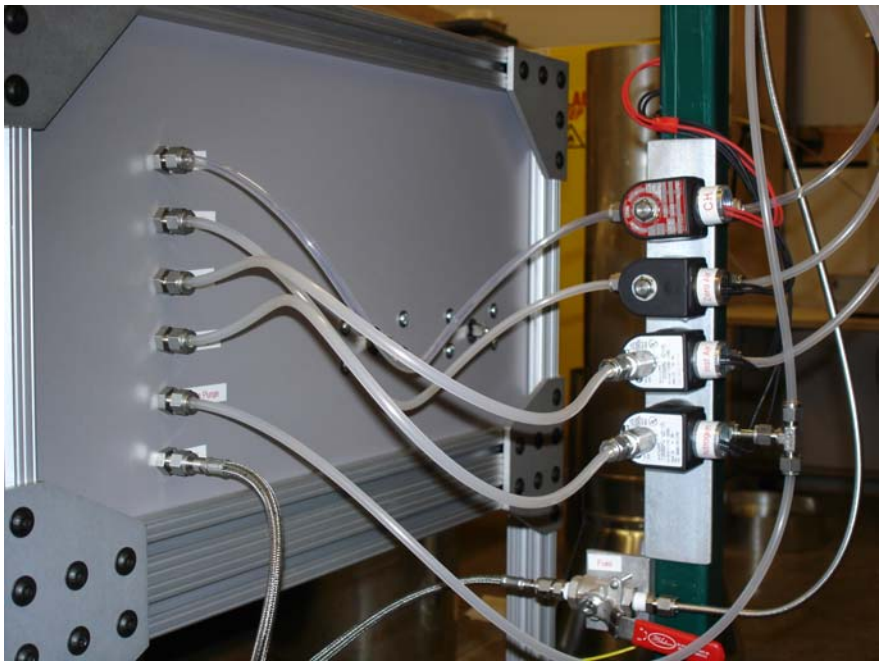

Figure 31: Solenoid valves controlling ignition and purge systems and their connection to the combustor stand.

Nitrogen Purge

Bottled nitrogen is used to provide an inert purge of both the fuel line and the emissions sample line. Purge of the fuel injector is critical to prevent coking or other sources of flow degradation. Similarly, the emissions probe must be cleared to prevent

buildup that may block sampling. Nitrogen is provided to purge the fuel system by the use of a four way union located on the combustor stand. One union connection provides fuel from the pump through the 1/4" line. Two of the connections provide fuel to the combustor through 1/8" stainless steel lines. The remaining connection provides the nitrogen. Both the nitrogen and fuel lines have check valves preventing backflow of nitrogen or fuel into the opposing systems.

The nitrogen supply is controlled by a normally-open Parker solenoid valve, wired through the SSR control board. Thus, when the test is stopped by either emergency, electrical outage or standard shutdown, power is cut from both the fuel line emergency valve and the nitrogen control valve. This cuts fuel pressure on the fuel line and engages the nitrogen line, purging the fuel injectors. Nitrogen is also supplied to the fuel line near the fuel emergency shutoff valve to purge the majority of the fuel line during maintenance.

The nitrogen supply is also connected to a UCI 3-way, pneumatically actuated valve. Two of these valves run in series along the emissions line and are actuated by a normally-open Parker solenoid valve, run through the SSR PB24 control board. Again, when power is cut to the solenoid valve it in turn actuates both three way valves pneumatically. This disconnects the emissions probe from the gas analyzer. Nitrogen flows to the emissions probe and purges it, the rest of the emissions line is opened to the atmosphere, through a filter, to allow for continued pumping by the gas analyzer system. Figure 32 details the fluid systems running throughout the laboratory.

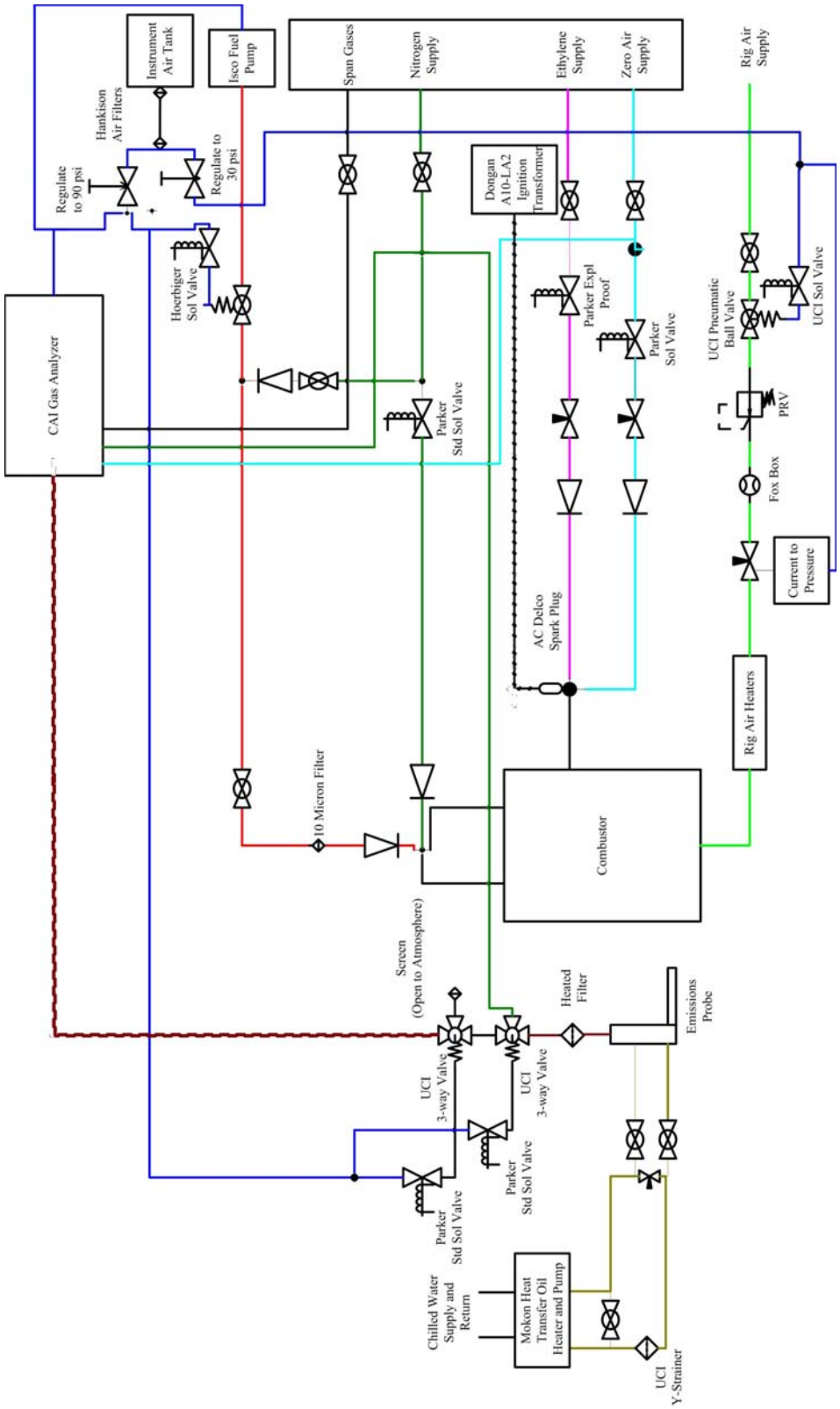

Figure 32: Liquid and gas systems in the laboratory.

Gas Analyzer

As discussed in previously, a California Analytical Instruments (CAI) Raw Emissions Test Bench is used to analyze combustor emissions for products of interest. These include total hydrocarbons (THC), nitrogen oxides (NOx), carbon dioxide (CO_2), carbon monoxide (CO), and oxygen (O_2), and are measured by a Model 300 HFID, a Model 400 HCLD, a Model 300 NDIR and a Model 300 paramagnetic oxygen detector respectively. The theory behind the operation of these detectors is covered in chapter two.

This emissions data must be taken reliably to produce useful results. The CAI gas detectors making up the test bench fall within specifications for raw emissions measurements as defined in SAE ARP 1256. (Dittman, 2006:23). The concentration of these gases is of interest to the experiment, as they are used to determine the emissions index, this in turn is used to determine the combustion efficiency.

The gas detectors require the use of calibration and span gases, purge air and hydrogen-helium fuel for calibration and operation. With the exception of the purge air, these substances are stored in compressed bottles outside of the laboratory building. The pressure is regulated to the desired value at the bottle location, and then flows into the laboratory through two bundles of seven 1/4" copper tubes. Purge air is provided through the instrument air system. The mixture, required flow rates, delivery pressures and other requirements for these gases are listed in Appendix A.

The CAI gas analyzer outputs the concentration of gases to digital displays mounted on the front of its body. However, for data recording purposes and ease of control this data is output by a 4-20mA signal to the DAQ and computer control system.

These signals are received by an NI 1303 Isothermal Terminal Block, and are displayed and recorded to file with proper scaling via the LabView software. This software also automatically controls the range setting of each detector. As seen in Table 3 the range setting of each detector enables it to provide good resolution on the actual concentration of the particular gas. Use of the G4PB24 solid-state relay board allows the computer to control the range remotely.

Table 3: Ranges for gases analyzed by CAI test bench.

Gas	Range	Span
Oxygen	1	0-5%
	2	0-10%
	3	0-25%
CO	1	0-2k ppm
	2	0-1%
CO_2	1	0-5%
	2	0-20%
NO_X	1	0-30 ppm
	2	0-100 ppm
	3	0-300 ppm
	4	0-1k ppm
	5	0-3k ppm
THC	1	0-10 ppm
	2	0-30 ppm
	3	0-100 ppm
	4	0-300 ppm
	5	0-1k ppm
	6	0-3k ppm
	7	0-10k ppm

Emissions Collection

The CAI gas analyzer receives the emissions from the combustor through the emissions collection system. Exhaust exiting the combustor is collected using a stainless steel exhaust probe. This probe (shown in Figure 33) has an approximately 1/8" diameter opening to collect emissions. Because of the high temperature of the exhaust stream, the

probe is built with an enclosed heat exchanger that circulates heat transfer oil at approximately 450K (350 °F) too cool the probe and maintain gas temperature.

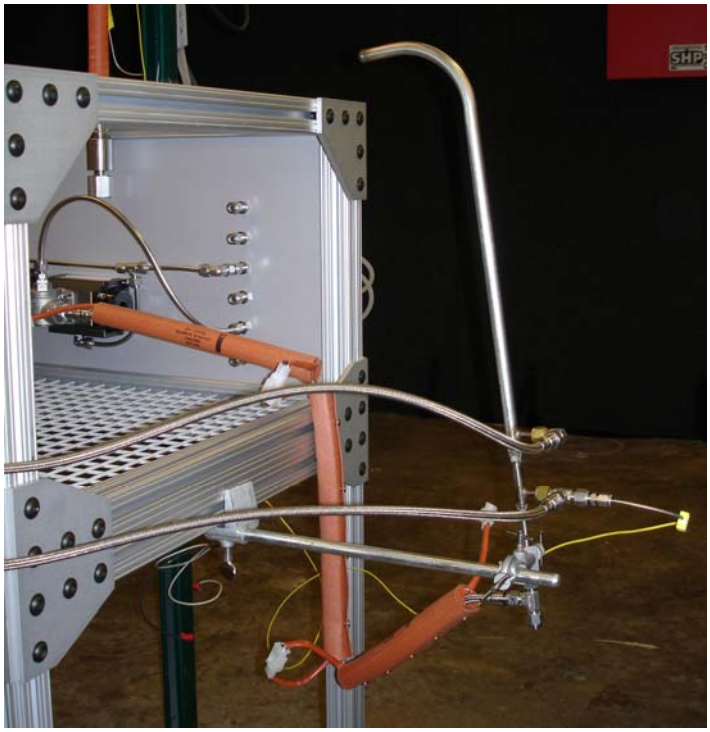

Figure 33: Oil heated emissions probe and electrically heated line on test stand.

According to SAE ARP 1256, the emissions sample must be maintained at 433K ± 15K (320°F ± 27 °F). This is to keep any water in a completely gaseous state as it may damage systems or skew data if it condenses in the sample line (SAE ARP 1256: Section 10.3). A Mokon H22103AJ Compact Heated Thermal Fluid System (shown in Figure 34) heats and circulates the oil at approximately 2.75 bar (40 psi). From the Mokon unit 3/8" stainless steel tubing provides oil supply and return lines. For proper operation of the Mokon system, a laboratory wide chilled water system is connected to the unit. This circulates a chilled water-glycol mixture at approximately 3.45 bar (50 psi) and 266K (20°F).

Traveling out of the Mokon unit, oil encounters a bypass with a metering valve. This provides a place for the oil to recirculate while the system is being warmed up to temperature and viscosity is high. It also passes through a Y-strainer on its way to the emissions probe. Near the probe, another bypass with a metering valve enables any necessary recirculation due to restriction in tube diameter at the probe. Ball valves on both lines allow for probe disconnect. The valves are connected to the probe by 3/16" flexible, stainless steel braided, Teflon tubing. This enables the probe to be easily positioned as required. The oil temperature is measured by a K-type thermocouple at the oil inlet to the probe for monitoring by the computer control system.

Figure 34: Mokon heater and pump unit for heat transfer oil used to cool emissions probe.

The sample gases exit the probe into a 1/4" piece of braided, flexible Teflon tubing to provide for probe positioning. The emissions then pass through two stainless steel UCI 3-way valves that actuate probe purging after experimentation is complete. These lines are exposed to the atmosphere, and thus use several Watlow electronic tube heaters to maintain gas temperature. As seen in Figure 35, a Watlow SD31 temperature

controller located at the computer station is used to maintain the tube heater's temperature. The control loop includes a solid-state relay and a K-type thermocouple.

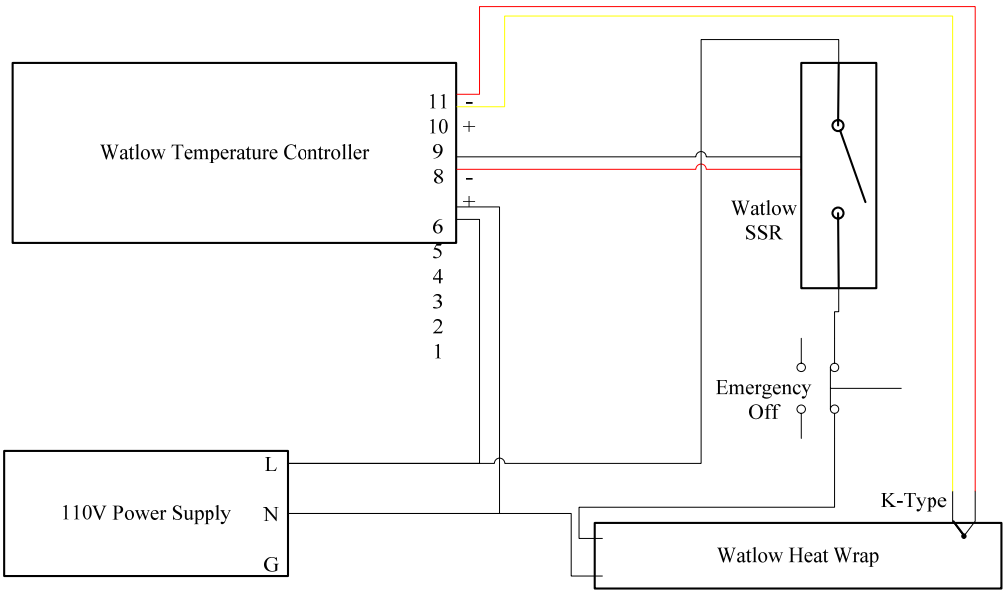

Figure 35: Temperature control loop of exposed emissions line.

After the 3-way valves the gas enters a Unique Products International heated gas filter and a 9 m (30 ft) heated line. The filter removes debris that may clog the transport line or damage analyzer components. Two additional Watlow SD31 temperature controllers also control the temperature of these systems. However, these are located in the CAI gas analyzer test bench. Thermocouples have been pre-manufactured into both items. The test bench also includes a pump that transports the gas from the probe to the analyzer.

Instrument Air

A Kaeser compressor located in Building 644 provides instrument air at 6.9 bar (100 psi). This air is used to energize all the pneumatically actuated valves, the current-to-pressure transmitter, and the syringe pump switching control. It also provides purge

air for the CAI gas analyzer. The use of instrument air from a distinct compressor prevents loss of control systems when air is drawn for use in the combustor. For further protection against control failure, the compressed air enters a large tank before being distributed. This provides a buffer for fluctuations in the supply line.

From the tank, the instrument air passes through two Hankison compressed air filters. These progressively remove oil and particulates from the air that may damage instruments and control valves. Two regulators then provide air at either 30 psi (for the current-to-pressure transmitter) or 90 psi (for all other equipment).

Combustor Stand

For mounting the combustor and providing maximum flexibility an 80/20 extruded aluminum stand was designed. This stand can mount a combustor system much larger than the one currently under investigation. A shelf level and mounting panel provide locations for support equipment such as the UCI 3-way valves, gas and fuel connections and the heated emissions filter.

Casters and wheels were constructed for the stand so it could be set on a pair of Unistrut rails bolted to the laboratory floor. Flexible connections for ethylene, zero air, nitrogen, instrument air and fuel are also made to the stand. This system enables the combustor to be moved for calibration of the laser system and then returned in a repeatable manner to the correct location. Adjustable stops in the Unistrut tracks make changes to the desired location possible.

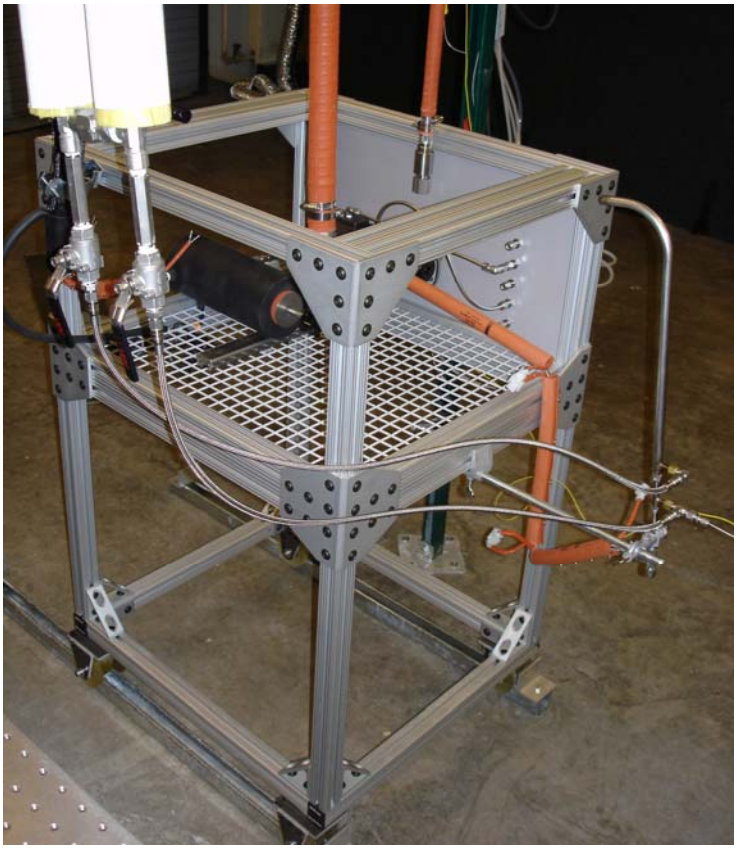

Figure 36: Combustor stand with exhaust probe assembly.

Exhaust System

To maintain a safe working environment, exhaust from the combustion system is carried away through an exhaust system. The system consists of mostly 16" diameter galvanized steel circular ductwork leading outside the building. A circular fan pulls air through the system at approximately 1.0 kg/s (1800 SCFM). This is sufficient to turn over the air in the laboratory four times an hour.

On the combustor side both an exhaust hood and a main exhaust catch are used. The square exhaust hood is positioned directly over the combustor and is 0.5 meters (20 inches) on each side. It contains an adjustable damper in line to control the amount of flow through itself. The catch is a stainless steel box, 0.3 meters (12 inches) on a side, positioned just beyond the combustor's main vane exhaust. Stainless steel circular

ductwork, 12” in diameter connects the box to the main line. The exhaust box contains several closable windows enabling optical access to the combustor.

Laser Diagnostic System

Innovative Scientific Solutions Incorporated (ISSI) designed and installed the advanced laser diagnostic system. As mentioned previously, this system enables the AFIT small-scale combustion facility to conduct instantaneous Raman, PIV, PLIF, LII and CARS diagnostics. The system is mounted on several movable optical breadboard tables located around the combustor. The system operates free of excess clutter thanks to the Unistrut frame.

The major components of the laser diagnostic system include:

- A dual-pulsed Nd:YAG laser that at 800mJ at 532nm wavelength produced by Spectra Physics.
- A pulse stretcher and two ICCD cameras with a 5.0 ns gate.
- Various optics, filters and lenses as appropriate to the diagnostic techniques.
- A rail and traverse system for location of the appropriate optics and cameras.
- A Continuum ND600 narrowband dye laser with frequency doubler.
- A broadband dye laser created by ISSI
- A computer system with the associated control and analysis software.

3.2 Real Combustor Design

Using the geometry developed by Moenter in his CFD work, a real combustor rig design for construction was necessary. Although the CFD model was finished, many details still needed to be worked out in order to make the combustor a reality. This included tasks such as: locating pressure and temperature taps, connectivity to the laboratory systems, injecting the fuel, locating and mounting quartz windows, material selection, air distribution to jets, and construction concerns.

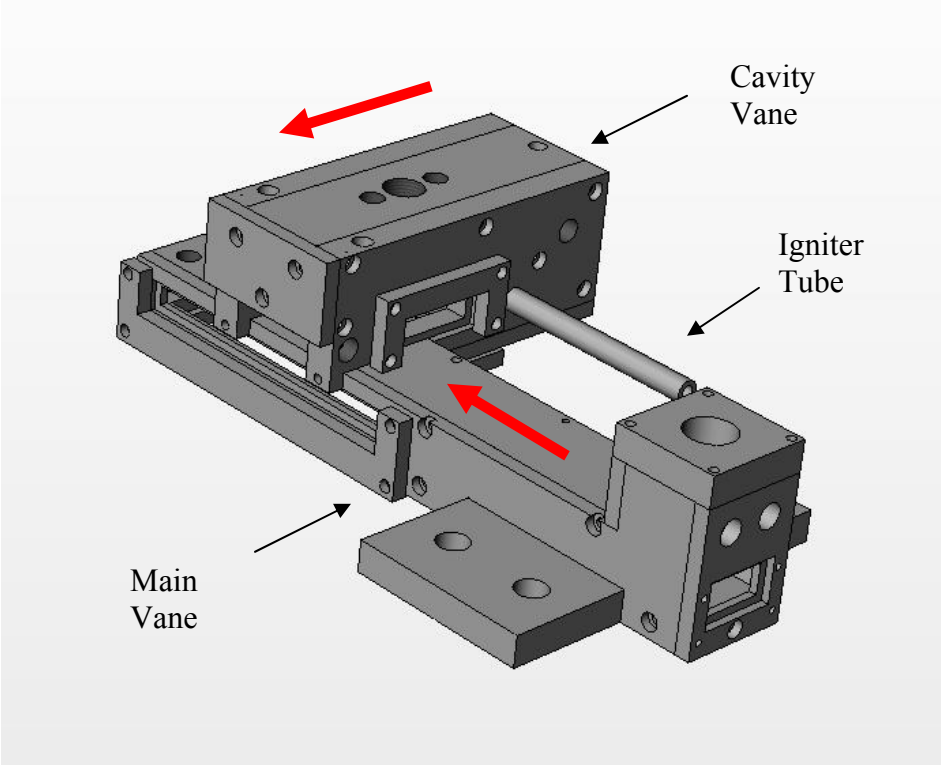

Figure 37: Flat combustor cavity design with main vane. Airflow direction is shown in red.

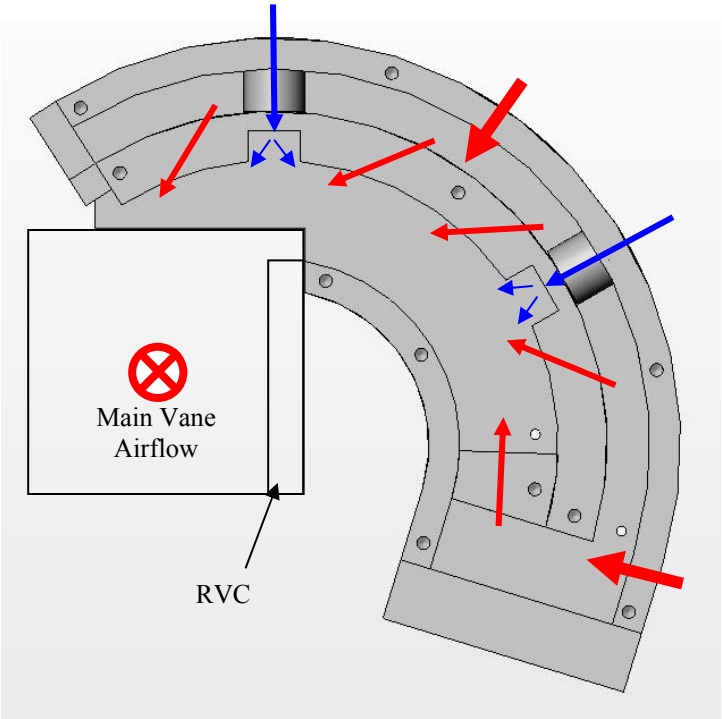

Figure 38: Cross-section of curved combustor cavity. Airflow is shown in red; fuel flow is shown in blue. The location of airflow through the main vane (moving into the page) and the radial vane cavity (RVC) is also indicated.

It was determined the rig should be built of type 316 stainless steel for strength at high temperature. Most of the parts are 0.25" and 0.50" stainless plates. It was also decided the device should be constructed using mechanical fastening. Specifically many socket head cap machine screws were employed. This enabled geometric location and fit to be more precise than welding, and better allows for thermal expansion. Sealing of the combustor with this method is not ideal, but is satisfactory.

Temperature at various locations in the combustor is measured by five K-type thermocouples. These can withstand the high temperatures involved. They are mounted using graphite ferrules locked in 1/16" stainless steel Swagelok connections. The ferrules allow the thermocouples to be adjusted in their mounts, while maintaining a good seal. Thermocouple locations are at the back of the cavity, the cavity exit, and the main vane entrance and exit. Four pressure taps are also mounted with 1/8" stainless steel Swagelok

connections. Several Dwyer 682 series pressure transducers and two Dwyer 655 series differential pressure transducers read pressure from these taps. Pressure taps are located directly across from all thermocouple locations.

Quartz windows, 0.3175 cm (1/8") in thickness, are mounted on the combustor in many locations to allow access to laser diagnostics. The mount is provided by recessed cavities in the combustor that locate the quartz while leaving 1/16" all around it to provide for differences in thermal expansion. The quartz is then sandwiched into position between the recessed cavity and another piece of stainless steel. The plate is compressed on the quartz using a screw-mounted spring. The window seals using a layer of high temperature Unifrax ceramic paper, 0.159 cm (1/16") in thickness.

As mentioned previously, two combustor rigs were developed; one uses a curved cavity geometry, the other a flat geometry. Testing and comparison of both rigs will allow for the isolation of the centrifugal effects on the combustor. The two rigs use the exact same main vane geometry, so the cavities are interchangeable with the same main vane section. This section cantilevers off the laboratories combustion stand to allow for maximum access.

Windows are located in the main vane across from and perpendicularly below the RVC cavity. Another window is located perpendicular to both the RVC windows, at the main vane entrance. Immediately across from this window is the main vane exhaust, open to the atmosphere. Windows in the laboratory's exhaust vent will allow for full access to the RVC cavity by laser diagnostics. The flat rig has two windows across from each other in the cavity section and one perpendicular to these windows on the bottom. This allows for a variety of diagnostic techniques to be employed in the cavity.

Fuel is injected into the rig using two Goodrich 46817-33 pressure-atomizing nozzles. The nozzles spray at a full cone angle of 80° and have a 0.3 flow number. This differs from the cone angles of the Moenter CFD models.

Ignition of the rig is in the cavity section, upstream of the first fuel injection point. A 3/8" stainless steel tube is welded to the cavity sidewall, and connected to the ethylene torch ignition system previously described. Fuel from the atomizers collects on the cavity's sidewall, and thus this torch location may be considered the most ideal place for ignition.

IV. Results and Discussion

The implementation of the facility design, along with innovative solutions developed during construction has resulted in a practical and flexible laboratory for AFIT to conduct combustion research. This was made possible by the selection of materials, systems and parts useful in any one of a variety of combustion research projects. The major capabilities of this design and the flexibility of the laboratory will be discussed in this section.

The combustor stand is oversized for the sectional combustor rigs for the purpose of future experiments. The use of the 80/20 extruded aluminum system provides plenty of strength for much larger systems. The particular combustion experiment can be designed to bolt onto the stand in a variety of ways through the use of the channels and T-nuts that are part of the 80/20 design. The track system not only provides for easy calibration, but also variable positioning as the experiment demands. The stand is also removable and exchangeable. All connections to the stand are Swagelok compression fittings and thus easily exchangeable or replaceable when necessary. Hot connections are treated with a nickel based anti-seize lubricant to ensure repeatable use and exchange.

The exhaust system provides significantly more airflow than is necessary for the UCC sectional rig experiments. The exhaust's ability to turn over the volume of room air several times an hour will ensure safety of those conducting experiments on systems much larger than those currently planned. The use of both an exhaust hood and a horizontal catch will also allow open and varying exhaust orientations such as in the planned UCC experiment.

The positioning of the stand and the exhaust capabilities make open flame experiments practical. This is necessary for a combustion facility as operating only enclosed experiments significantly reduces the amount of research that can be done. This capability opens up a wide variety of possible uses including rocket motors, burners and other open flame phenomena.

The use of two combustor rig airlines of differing sizes was necessary to research of the UCC. It also allows flexibility in future experiments where two independently controlled airlines are needed. As mentioned previously the main line is intended to provide up to 0.12 kg/s (200 SCFM), and the secondary 0.03 kg/s (60 SCFM) of air. Based on these values and the possible flow rates of the fuel pump, equivalence ratios for JP-8 can be obtained for maximum airflow. The main line ranges from 0.0018 to 1.3 and the secondary can vary from 0.0061 to 4.3. The variable heating of this air up to 530K (500°F), or 670K (750°F) without the use of the flexible connection hoses, is also useful for a range of experimental conditions.

The use of the California Analytical Instruments gas analyzer and supporting hardware allows the laboratory to conform to the testing standards laid out in the SAE ARP 1256. The analyzer's uncertainty and drift are within acceptable ranges of the standards. The heated emissions transport line and heated filter are part of the CAI system. The heated valves and lines provided by the laboratory design near the probe, and the hot oil system also allows these standards to be maintained. This makes the facility fully capable of gas emission sampling up to standard.

The computerized control of the lab and use of the National Instruments hardware and LabView software is another advantage of the system. The NI products are

commonly used for data acquisition in a variety of laboratories across the country. The LabView graphical programming software is relatively easy to learn, use and manipulate. As the majority of the systems are based on computer control, setup for a differing experiment may be accomplished simply by software modification. Use of computer-controlled valves allows the lab operation to be literally programmed as desired. Remote ignition, purging and emergency shutoff allow involved experiments to be conducted, with little concern for potentially complex laboratory operations. Finally, all of the associated control hardware has much more connectivity than is currently being used. This means the addition of more systems to the laboratory would be easily accomplished.

The capabilities of the base laboratory systems are enhanced greatly by the installation of the advanced laser diagnostics system. This system will allow any knowledgeable user of the laboratory to conduct state-of-the-art combustion research. The accessibility provided by the combustor stand and exhaust design will allow laser use in almost any orientation. The system will allow studies of the flame and exhaust in regards to point and planar studies of species concentration, temperature, soot location, flame location, and velocity fields.

V. Conclusions

5.1 Overview of Project

The AFIT small-scale combustion facility is complete and its first experiment designed and built. Starting with existing design and construction of much of the facility by Dittman, new designs and specifics for the completion of the facility were developed. Purchasing of parts and construction was then completed. A design for two sectional combustor rigs, one with a curved cavity and one flat were created based on the CFD work of Moenter. The flat rig design was constructed. It will provide the inaugural test in the laboratory. Documentation and organization of the laboratory for future modification and operation were also completed. Finally, an accessible but detailed investigation into the basics of the combustion laser diagnostics available for use in this laboratory was conducted.

The facility gives future researchers the ability to perform open flame or contained combustion experiments with great flexibility. Two independently controlled air lines provide heated air at different flow rates. The air can be delivered at up to 530 K (500°F) at 0.12 kg/s (200 SCFM) for the large line and 0.03 kg/s (60 SCFM) for the smaller. The air is delivered at nearly atmospheric pressure. Two syringe pumps continuously provide liquid fuel at up to 5.67 mL/s.

Emissions sampling and testing is provided within standards as defined by SAE ARP 1256. Use of oil cooling and electrical heating maintains sample temperature as prescribed during transport to equipment meeting testing standards. Thus, the results of any emissions tests conducted by the facility are given credibility. Additional data is provided by several systems. The simplest of these are strategically placed

thermocouples and pressure taps for recording of point temperature and pressure values. A humidity transmitter also gives water content of incoming rig air.

The installation of an advanced laser combustion diagnostics system will provide a wealth of possibilities to the researcher. This system will be capable of conducting instantaneous Raman, Raman spectroscopy, CARS, PLIF and LII measurements. These allow both point and planar measurements of species concentration; temperature, velocity, soot location and combustion location to be assessed.

The facility is centrally controlled and data is automatically taken through a computer control station. Routing of electrical control and information systems through this station provides for safe and simple control of the laboratory. Thus, the researcher can concentrate on the experiment itself while easily accessing controls from a single location. This station also uses data acquisition software and hardware enabling modification for a variety of tests.

5.2 Future Work and Recommendations

Several steps will be necessary to bring the system fully online. Minor parts for the completion of the combustor stand, installation of the gases and construction of the flat UCC rig are currently on order but have not yet arrived. Construction of the laser system and the exhaust system is currently being completed. A live fire has not been conducted and adjustments may have to be made as a result of the first few tests. This will likely result in a more detailed operating checklist as well. When firm dates for testing are established the ordering of calibration, span and fuel gases along with JP-8 must be completed.

All aspects of the system that are fully in place have been tested and are prepared for use in research on the UCC flat sectional combustor rig. All valve control systems are operating correctly, and the rig air system has been validated. Pressures and temperature readings are reasonable, as is data from the gas analyzer. Remote range selection on the analyzer by the computer station operates correctly. Signal readings from all other devices are also working correctly. The emissions transport system and combustor stand equipment is operating properly.

It is suggested research begins with a study of the UCC flat sectional rig's exhaust by use of the emissions probe and gas analyzer. The laboratory is currently prepared for this configuration and the rig will be soon completed. Running this test will enable validation of the system in an actual experiment, and provide good data for investigation of the UCC. It is also suggested that OH PLIF studies of a calibration device (such as a Hankin burner) be conducted to validate the laser diagnostic system. These two experiments will give the facility and researcher a good grounding for future work.

Appendix A: System Technical Information

Table 4: Wiring code for NI SCXI 1100 DAQ measurement and control system.

SCXI 1100 Slot Location	NI Module	NI Terminal Block	NI Channel #	Enclosure Terminal Block Connection #	Polarity	Instrument Connection #	Description of Instrument Connection
1	SCXI 1102	SCXI1303	CH0+	ETB A - 1	+	CAI TB3-1	California Analytical Instruments (CAI)
1	SCXI 1102	SCXI1303	CH0-	ETB A - 2	-	CAI TB3-2	THC Analyzer Output (4-20mA DC)
				ETB A - 3	Ground		
1	SCXI 1102	SCXI1303	CH1+	ETB A - 4	+	CAI TB3-7	THC Oven Temperature (1 mV/°C)
1	SCXI 1102	SCXI1303	CH1-	ETB A - 5	-	CAI TB3-8	
				ETB A - 6	Ground		
1	SCXI 1102	SCXI1303	CH2+	ETB A - 7	+	CAI TB3-18	NOx Analyzer Output (4-20mA DC)
1	SCXI 1102	SCXI1303	CH2-	ETB A - 8	-	CAI TB3-19	
				ETB A - 9	Ground		
1	SCXI 1102	SCXI1303	CH3+	ETB A - 10	+	CAI TB3-24	NOx Conv Temperature (10 mV/°C)
1	SCXI 1102	SCXI1303	CH3-	ETB A - 11	-	CAI TB3-25	
				ETB A - 12	Ground		
1	SCXI 1102	SCXI1303	CH4+	ETB A - 13	+	CAI TB3-27	NOx Oven Temperature (10 mV/°C)
1	SCXI 1102	SCXI1303	CH4-	ETB A - 14	-	CAI TB3-28	
				ETB A - 15	Ground		
1	SCXI 1102	SCXI1303	CH5+	ETB A - 16	+	CAI TB3-37	CO2 Analyzer Output (4-20mA DC)
1	SCXI 1102	SCXI1303	CH5-	ETB A - 17	-	CAI TB3-38	
				ETB A - 18	Ground		
1	SCXI 1102	SCXI1303	CH6+	ETB A - 19	+	CAI TB3-45	CO Analyzer Output (4-20mA DC)
1	SCXI 1102	SCXI1303	CH6-	ETB A - 20	-	CAI TB3-46	
				ETB A - 21	Ground		
1	SCXI 1102	SCXI1303	CH7+	ETB A - 22	+	CAI TB3-53	O2 Analyzer Output (4-20mA DC)
1	SCXI 1102	SCXI1303	CH7-	ETB A - 23	-	CAI TB3-54	
				ETB A - 24	Ground		
1	SCXI 1102	SCXI1303	CH25+	ETB A - 29	+	1+	Viasala Dewpoint Transmitter Output
1	SCXI 1102	SCXI1303	CH25-	ETB A - 30	-	1-	(4-20mA DC)

Table 4: Wiring code for NI SCXI 1100 DAQ measurement and control system. (continued)

SCXI 1100 Slot Location	NI Module	NI Terminal Block	NI Channel #	Enclosure Terminal Block Connection #	Polarity	Instrument Connection #	Description of Instrument Connection
2	SCXI 1102	SCXI1303	CH0+	ETB A - 27	+	PT 1	(PT 1) Main Line pressure before dome loader,
2	SCXI 1102	SCXI1303	CH0-	ETB A - 28	-	-1	Pressure Tranducer Box 1 (4-20mA DC)
2	SCXI 1102	SCXI1303	CH1+	ETB C -1	+	Ch	(TC 1) Main Line temperature before dome loader
2	SCXI 1102	SCXI1303	CH1-	ETB C - 1	-	A1	(K Type TC)
2	SCXI 1102	SCXI1303	CH2+	ETB A - 31	+	PT 2	(PT 2) Main Line Pressure at combustor inlet,
2	SCXI 1102	SCXI1303	CH2-	ETB A - 32	-	-2	Pressure Transducer Box 1 (4-20mA DC)
2	SCXI 1102	SCXI1303	CH3+	ETB A - 33	+	TS1 -	Main Line temperature from Fox Box 1
2	SCXI 1102	SCXI1303	CH3-	ETB A - 34	-	TS2 4-	(4-20mA DC)
2	SCXI 1102	SCXI1303	CH4+	ETB A - 35	+	2A+	Main Line Flow from 2404 PID Controller
2	SCXI 1102	SCXI1303	CH4-	ETB A - 36	-	2B-	(4-20mA DC) (Retransmitted from Fox Box 1)
2	SCXI 1102	SCXI1303	CH5+	ETB A - 37	+	14	Main Line temperature from heater controller UT420
2	SCXI 1102	SCXI1303	CH5-	ETB A - 38	-	15	(4-20mA DC)
2	SCXI 1102	SCXI1303	CH6+	ETB A - 39	+	PT 4	(PT 4) Main Line pressure difference across
2	SCXI 1102	SCXI1303	CH6-	ETB A - 40	-	-4	combustor, Pressure Transducer Box 1 (4-20mA DC)
2	SCXI 1102	SCXI1303	CH7+	ETB C - 2	+	Ch	(TC 2) Main Line temperature at combustor inlet
2	SCXI 1102	SCXI1303	CH7-	ETB C - 2	-	A1	(K Type TC)
2	SCXI 1102	SCXI1303	CH8+	ETB A - 43	+	PT 3	(PT 3) Secondary Line pressure before dome loader,
2	SCXI 1102	SCXI1303	CH8-	ETB A - 44	-	-3	Pressure Transducer Box 1 (4-20mA DC)
2	SCXI 1102	SCXI1303	CH9+	ETB C - 3	+	Ch	(TC 3) Secondary Line temperature before dome
2	SCXI 1102	SCXI1303	CH9-	ETB C - 3	-	A1	loader (K Type TC)
2	SCXI 1102	SCXI1303	CH10+	ETB A - 47	+	PT 6	(PT 6) Secondary Line Pressure at combustor inlet,
2	SCXI 1102	SCXI1303	CH10-	ETB A - 48	-	-6	Pressure Transducer Box 2 (4-20mA DC)
2	SCXI 1102	SCXI1303	CH11+	ETB A - 49	+	TS1 -	Secondary Line temperature from Fox Box 2
2	SCXI 1102	SCXI1303	CH11-	ETB A - 50	-	TS2 4-	(4-20mA DC)
2	SCXI 1102	SCXI1303	CH12+	ETB A - 51	+	2A+	Secondary Line Flow from 2404 PID Controller
2	SCXI 1102	SCXI1303	CH12-	ETB A - 52	-	2B-	(4-20mA DC) (Retransmitted from Fox Box 2)
2	SCXI 1102	SCXI1303	CH13+	ETB A - 53	+	14	Secondary Line temperature from heater controller
2	SCXI 1102	SCXI1303	CH13-	ETB A - 54	-	15	UT420 (4-20mA DC)
2	SCXI 1102	SCXI1303	CH14+	ETB A - 55	+	PT5	(PT 5) Secondary Line pressure difference across
2	SCXI 1102	SCXI1303	CH14-	ETB A - 56	-	-5	combustor, Pressure Transducer Box 1 (4-20mA DC)
2	SCXI 1102	SCXI1303	CH15+	ETB C - 4	+	Ch	(TC 4) Secondary Line temperature at combustor
2	SCXI 1102	SCXI1303	CH15-	ETB C - 4	-	A1	inlet (K Type TC)
2	SCXI 1102	SCXI1303	CH16+	ETB A - 59	+	PT8	(PT 8) Liquid Fuel Pressure, Pressure Transducer
2	SCXI 1102	SCXI1303	CH16-	ETB A - 60	-	-8	Box 2 (4-20mA DC)
2	SCXI 1102	SCXI1303	CH17+	ETB C - 5	+	Ch	(TC 5) Liquid Fuel Temperature from thermocouple
2	SCXI 1102	SCXI1303	CH17-	ETB C - 5	-	A1	(K Type TC)
2	SCXI 1102	SCXI1303	CH18+	ETB C - 6	+	Ch	(TC 6) Oil Temperature from thermocouple
2	SCXI 1102	SCXI1303	CH18-	ETB C - 6	-	A1	(K Type TC)
2	SCXI 1102	SCXI1303	CH19+	ETB A - 65	+	PT9	(PT 9) Ambient pressure,
2	SCXI 1102	SCXI1303	CH19-	ETB A - 66	-	-9	Pressure Transducer Box 2 (4-20mA DC)
2	SCXI 1102	SCXI1303	CH24+	ETB C - 8	+	Ch	(TC 8) Main Line temperature at combustor exit
2	SCXI 1102	SCXI1303	CH24-	ETB C - 8	-	A1	(K Type TC)
2	SCXI 1102	SCXI1303	CH25+	ETB C - 9	+	Ch	(TC 9) Secondary Line temperature at combustor
2	SCXI 1102	SCXI1303	CH25-	ETB C - 9	-	A1	inlet (K Type TC)
2	SCXI 1102	SCXI1303	CH26+	ETB C - 10	+	Ch	(TC 10) Cavity back wall temperature (K Type TC)
2	SCXI 1102	SCXI1303	CH26-	ETB C - 10	-	A1	
2	SCXI 1102	SCXI1303	CH29+	ETB A - 67	+		Gaseous Fuel Flow (for future use)
2	SCXI 1102	SCXI1303	CH29-	ETB A - 68	-		
2	SCXI 1102	SCXI1303	CH30+	ETB A - 69	+	PT7	(PT 7) Gaseous Fuel Pressure,
2	SCXI 1102	SCXI1303	CH30-	ETB A - 70	-	-7	Pressure Transducer Box 2 (4-20mA DC)
2	SCXI 1102	SCXI1303	CH31+	ETB C - 7	+	Ch	(TC 7) Gaseous Fuel Temperature from thermocouple
2	SCXI 1102	SCXI1303	CH31-	ETB C - 7	-	A1	(K-Type TC)

Table 4: Wiring code for NI SCXI 1100 DAQ measurement and control system. (continued)

SCXI 1100 Slot Location	NI Module	NI Terminal Block	NI Channel #	Enclosure Terminal Block Connection #	Polarity	Instrument Connection #	Description of Instrument Connection
6	SCXI 1124	SCXI 1325	CH0 SUPPLY	ETB A - 79	+	3A	Main Line Flow PID Setpoint to 2404 PID Controller
6	SCXI 1124	SCXI 1325	CH0 ISINK	ETB A - 80	-	3D	
6	SCXI 1124	SCXI 1325	CH1 SUPPLY	ETB A - 81	+	3A	Secondary Line Flow PID Setpoint to 2404 PID
6	SCXI 1124	SCXI 1325	CH1 ISINK	ETB A - 82	-	3D	Controller
6	SCXI 1124	SCXI 1325	CH2 SUPPLY	ETB A - 83	+	21	Main Line Heater Controller Setpoint to UT420
6	SCXI 1124	SCXI 1325	CH2 ISINK	ETB A - 84	-	22	
6	SCXI 1124	SCXI 1325	CH3 SUPPLY	ETB A - 85	+	21	Secondary Line Heater Controller Setpoint to UT420
6	SCXI 1124	SCXI 1325	CH3 ISINK	ETB A - 86	-	22	

Table 5: Wiring code for Opto 22 PB24 solid state relay board used for control of systems throughout the room.

Relay #	Connection #	Type		Device connected
0	1	ODC5R		Main Air Valve
0	2			
1	3	ODC5R		Secondary Air Valve
1	4			
2	5	ODC5R		Fuel Shutoff Valve
2	6			
3	7	ODC5R		
3	8			
4	9	ODC5A	+	Main Heater Emergency Shutoff
4	10		-	
5	11	ODC5A	+	Secondary Heater Emergency Shutoff
5	12		-	
6	13	ODC5A		
6	14			
7	15	ODC5A		
7	16			
8	17	OAC5A		Ethylene and Air Valves
8	18			
9	19	OAC5A		Torch Ignitor
9	20			
10	21	OAC5A		Probe purge
10	22			
11	23	OAC5A		Fuel Purge
11	24			
12	25	OAC5A		
12	26			
13	27	OAC5A		
13	28			
14	29	Empty		
14	30			
15	31	Empty		
15	32			
16	33	IDC5		
16	34			
17	35	IDC5		
17	36			
18	37	IDC5		
18	38			
19	39	IDC5		
19	40			
20	41	IAC5		Mushroom Button
20	42			
21	43	IAC5		Pressure Switch (exhaust system)
21	44			
22	45	IAC5		
22	46			
23	47	IAC5		
23	48			

Table 6: Wiring and digital channel code for Opto 22 G4PB24 optically isolated solid-state relay board used for controlling range selection on the raw emissions test bench.

Opto 22 G4PB24 Connection #	Enclosure Terminal Block Connection #	CAI Analyzer Rack Connection #	CAI Control Description	50 Pin Connector Line #	DAQ Pad-6508 Port and Channel
46	ETB B - 1	58	Oxygen Range 3 (0-25%)	3	CPC(8):6
44	ETB B -2	57	Oxygen Range 2 (0-10%)	5	CPC(8):5
42	ETB B - 3	56	Oxygen Range 1 (0-5%)	7	CPC(8):4
41,43,45	ETB B - 4	59	Oxygen Remote	7,5,3	CPC(8):4-6
40	ETB B - 5	49	CO Range 2 (0-1%)	9	CPC(8):3
38	ETB B - 6	48	CO Range 1 (0-2k ppm)	11	CPC(8):2
37,39	ETB B - 7	51	CO Remote	11,9	CPC(8):2-3
36	ETB B - 8	41	CO2 Range 2 (0-20%)	13	CPC(8):1
34	ETB B - 9	40	CO2 Range 1 (0-5%)	15	CPC(8):0
33,35	ETB B - 10	42	CO2 Remote	15,13	CPC(8):0-1
26	ETB B - 11	34	NOx Range 5 (0-3k ppm)	23	CPB(7):4
24	ETB B - 12	33	NOx Range 4 (0-1k ppm)	25	CPB(7):3
22	ETB B - 13	32	NOx Range 3 (0-300 ppm)	27	CPB(7):2
20	ETB B - 14	62	NOx Range 2 (0-100 ppm)	29	CPB(7):1
18	ETB B - 15	61	NOx Range 1 (0-30 ppm)	31	CPB(7):0
17,19,21,23,25	ETB B - 16	35	NOx Remote	31,29,27,25,23	CPB(7):0-4
14	ETB B - 17	68	THC Range 7 (0-10k ppm)	35	CPA(6):6
12	ETB B - 18	15	THC Range 6 (0-3k ppm)	37	CPA(6):5
10	ETB B - 19	14	THC Range 5 (0-1k ppm)	39	CPA(6):4
8	ETB B - 20	13	THC Range 4 (0-300 ppm)	41	CPA(6):3
6	ETB B - 21	67	THC Range 3 (0-100 ppm)	43	CPA(6):2
4	ETB B - 22	66	THC Range 2 (0-30 ppm)	45	CPA(6):1
2	ETB B - 23	69	THC Range 1 (0-10 ppm)	47	CPA(6):0
1,3,5,7,9,11,13	ETB B - 24	16	THC Remote	47,45,43,39,37,35	CPA(6):0-6

Table 7: Type, concentration and connection for all laboratory gases.

Gas type	Connection	Purpose	Pressure (psig)	Flowrate (lpm)
Air	CAI Purge	instrument air/purge air for 300 (CO_2, CO, O_2)	90	25
Air	CAI Zero Air/ combustor	zero air, oxidizer for 300 HFID burner (HC's) and ethylene torch	30	
CO	CAI CO-S2	span gas - high concentration		1
CO	CAI CO-S1	span gas - low concentration		1
CO_2	CAI CO_2-S2	span gas - high concentration		1
CO_2	CAI CO_2-S1	span gas - low concentration		1
C_3H_8 (propane)	CAI THC-S2	span gas - high concentration	30	
NO	CAI NO_x-S2	span gas - high concentration	25	
N_2	CAI N_2	cal gas / purge sample probe and fuel lines		1 to 2
O_2	CAI O_2	span gas		1 + - 0.5
40%H_2/60%He C3	CAI fuel	fuel for 300 HFID burner (HC's)	see comments	see comments
C_2H_4 (ethylene)	combustor	combustor ignition	30-40	

Gas type	Comments and Specs from CAI Manual	Ordered Concentration
Air	taken from filtered shop air, clean, dry, oil free	in house
Air	maximum 1 ppm C // minimum 3000ppm O_2 // maximum 1ppm NOx at 0.5 lpm, 25 psig	Zero Air
CO	minimum of 80% of range	4800 ppm w/ N_2 balance
CO	minimum of 80% of range	1600 ppm w/ N_2 balance
CO_2	minimum of 80% of range	9.1% w/ N_2 balance
CO_2	minimum of 80% of range	4.75% w N_2 balance
C_3H_8 (propane)		900 ppm C_3H_8 w/ N_2 bal
NO	w/ N_2 balance	98.2ppm NO, 0.4 ppm NO_2 w/ N_2 bal
N_2	w/o moisture or carbon compounds	N_2
O_2	maximum of 1 micron particle size (filter included in CAI sys) minimum of 80% of range	5% O_2 w/ N_2 bal
40%H_2/60%He C3	for burn Fuel @ 6.0/128 PSI/cc + Air @ 6.0/229 PSI/cc // for ignition Fuel: 5.8/124 PSI/cc	40%H_2/60%He
C_2H_4 (ethylene)		C_2H_8

Table 8: Compiled list of major equipment and technical data by system.

Air Heater	Model	Serial #	Line	Use	Outlet Temp	Power Limits
Gaumer	CS5F9N884YKWJ	05-11326	480V, 3 Phase	Heats main line combustor rig air	up to 538 °C (1000 F)	37.5 kW
Gaumer	C2P3N64M4KWJ	05-11326	480V, 3 Phase	Heats combustor rig air	up to 538 °C (1000 F)	12.3 kW
Current to Pressure Transmitter	Model	Serial #	Range	Use	Accuracy	Pressure Limits
Moore Industries	IPT[2]	1725762	0.21-1.03 bar (3-15 psig)	Takes signal from process controller and converts to pressure value for the needle valves	±0.1% of output pressure	Supply pressure must be 5 psi greater than upper signal, 20 to 40 psi
Flow Meters	Model	Serial #	Range	Use	Accuracy	Pressure Limits
Fox Thermal Instruments	FT2	W749	0-7.0 kg/min	Measure air flow in main line	±1% of reading	20.68 bar (300 psi)
	FT3	W382	0-2.0 kg/min	Measure air flow in secondary line	±1% of reading	20.68 bar (300 psi)
Fuel Atomizers	Model	Serial #	Press Loss	Use	Flow Number	Pressure Limits
Goodrich	Peanut tip pressure atomizer 46817-33	n/a	6.89 bar (100 psi) at 0.0037 kg/s (0.5 lbm/min) of fuel	Filters fuel to pump and combustor	0.3	n/a
Fuel Filters	Model	Serial #	Press Loss	Use	Filtration	Pressure Limits
Mott	6610-.170-10 (10 micron) 6610-.170-40 (40 micron)	6066101-100 6066101-400	n/a	Filters fuel to pump and combustor	10 and 40 micron respectively	n/a

Table 8: Compiled list of major equipment and technical data by system. (continued)

Fuel Pump System	Model	Serial #	Range	Use	Accuracy	Pressure Limits
ISCO	ISCO 1000D syringe Pump	A	1 to 408mL/min (6.8 mL/s)	Liquid Fuel delivery	±0.5% of flow	137.9 bar
	ISCO 1000D syringe Pump	B	1 to 408mL/min (6.8 mL/s)	Liquid Fuel delivery	±0.5% of flow	137.9 bar
Gas Analyzer	Model	Serial #	Range	Use	Accuracy	Pressure Limits
California Analytical Instruments	Model 300-HFID	P10009	0-10k ppm in 7 ranges	Hydrocarbon detection	Better than ±0.5% of full scale	n/a
	Model 400 HCLD	P10010	0-3k ppm in 5 ranges	Oxides of Nitrogen detection	Better than ±1% of full scale	n/a
	Model 300 CO and CO2 infrared analyzer	P09022	CO: 0-20% in 2 ranges CO2: 0-0.2% in 2 ranges	CO and CO2 detection	Better than ±1% of full scale	n/a
	Model 300 paramagnetic O2 analyzer	P09022	0-25% in 3 ranges	O2 detection	Better than ±1% of full scale	n/a
Gaseous Fuel Meter (for use in future work)	Model	Serial #	Range	Use	Accuracy	Pressure Limits
Brooks Intrument	Model 5853	105090294658001	0-200 SLPM	Controls the flow of gaseous fuel	±1% of full scale	100 bar

Table 8: Compiled list of major equipment and technical data by system. (continued)

Heated Oil system	Model	Serial #	Line	Use	Outlet Temp	Pressure Limits
MOKON	MOKON H22103AJ Heated Thermal Fluid System	7000363	220 V, 3 phase	To maintain the emission sample at 320 °F	Chiller water temperature to 177 °C (350 °F)	3.45 bar (50 psi) discharge pressure
Humidistat	Model	Serial #	Range	Use	Accuracy	Pressure/Temp Limits
Viasala	DMT348	B3510004	0-70% RH	Measures relative humidity of incoming air	±0.004%RH +20% of reading	40 bar/ 80 °C
Instrument Air Filters	Model	Serial #	Range	Use	Accuracy	Pressure Limits
	HF9-20-4DPL	0301	105 m^3/hr @ 7 kgf/cm^2 (60 SCFM @ 100psig)	rough inst air filter	mechanical seperator and 3 micron coalescer	17.24 bar (250 psig) @ 66 °C
Hankison	HF5-20-4DPL	0602	105 m^3/hr @ 7 kgf/cm^2 (60 SCFM @ 100psig)	fine/oil inst air filter	High effic (99.99%) coalescer	17.24 bar (250 psig) @ 66 °C
Needle Valves	Model	Serial #	Range	Use	Accuracy	Pressure Limits
Badger Meter	Research Control Valves	48072200101	n/a	Main line control	n/a	103.42 bar (1500 psi)
	Research Control Valves	48072200701	n/a	Secondary line control	n/a	103.42 bar (1500 psi)

Table 8: Compiled list of major equipment and technical data by system. (continued)

Pneumatic Ball Valves	Model	Serial #	Actuation Pressure	Use	Temp Limits	Pressure Limits
	PC/S2S-3	n/a	5.52 to 8.27 bar (80 to 120 psig)	Fuel line shutoff	n/a	n/a
	P0/B2F-12D1 P0/B2F-6D1	n/a	5.52 to 8.27 bar (80 to 120 psig)	Rig air shutoffs (main and sec)	n/a	n/a
	PS/S2S-2TT	n/a	5.52 to 8.27 bar (80 to 120 psig)	emissions line purge	182° C (360 °F) on seats and seals (Viton)	n/a
UCI	PS/S2S-2TT	n/a	5.52 to 8.27 bar (80 to 120 psig)	emissions line air feed	182 °C (360 °F) on seats and seals (Viton)	n/a
Pressure Reducing Valve	Model	Serial #	Range	Use	Accuracy	Pressure Limits
CASHCO	1/2" NPT DA3	AA4098-001-06	0-27.58 bar (0-400 psig)	Change pressure in the main line	n/a	27.58 bar (400 psi)
	1/2" NPT DA3	AA4098-001-05	0-27.58 bar (0-400 psig)	Change pressure in the secondary line	n/a	27.58 bar (400 psi)

Table 8: Compiled list of major equipment and technical data by system. (continued)

Pressure Transducers	Model	Serial #	Range	Use	Accuracy	Pressure Limits
Dwyer	682-3	2649303	0-17.24 bar (0-250 psig)	Main line pressure	±0.13% of full scale	34.5 bar (500 psi)
	682-3	2649304	0-17.24 bar (0-250 psig)	Secondary line pressure	±0.13% of full scale	34.5 bar (500 psi)
	682-0	2623272	1.72 bar (0-25 psig)	Main line plenum	±0.13% of full scale	6.89 bar (100 psi)
	682-0	2673169	1.72 bar (0-25 psig)	Secondary line plenum	±0.13% of full scale	6.89 bar (100 psi)
	655-5	n/a	0-0.07 bar (0-1 psi) diff	Main line combustor differential	±0.5% of full scale	20.68 bar (300 psi) continuous
	655-5	n/a	0-0.07 bar (0-1 psi) diff	Secondary line combustor differential	±0.5% of full scale	20.68 bar (300 psi) continuous
	682-1	2518196	0-3.45 bar (0-50 psig)	Liquid fuel pressure at combustor	±0.13% of full scale	10.34 bar (150 psi)
	682-4	2633896	0-34.5 bar (0-500 psig)	Gaseous fuel pressure at combustor	±0.13% of full scale	68.9 bar (1000 psi)
Omega	PX305-015AI	n/a	0-1.03 bar (0-15 psia)	Ambient pressure	±0.25% of full scale	n/a
Process Controllers	Model	Serial #	Line	Use	Accuracy	Power Limits
Eurotherm	2404 Control Setpoint Programmer	2404/NSGC/D6/D6/D5/Left	85-264 VAC	Controls the flow in the Main air line	±0.2% of max	15 Watt max
	2404 Control Setpoint Programmer	2404/NSGC/D6/D6/D5/Right	85-264 VAC	Controls the flow in the Secondary air line	±0.2% of max	15 Watt max
Watlow	SD31 Temperature Controller	n/a	85-264 VAC	Controls the stand emiss line temp	±0.1% of span	10 VA max

Table 8: Compiled list of major equipment and technical data by system. (continued)

Solenoid Valves	Model	Serial #	Line	Use	Pressure Limits	Power Limits
	71215SN2MN00H111P3	n/a	120 VAC	Ethylene control	10.34 bar (150 psig)	10 Watt max
	71215SN2MN00N0C111P3	n/a	120 VAC	Torch air control	10.34 bar (150 psig)	10 Watt max
	71295SN2KNJ1N0C111P3	n/a	120 VAC	Instrument air to UCI 3 ways	10.34 bar (150 psig)	10 Watt max
Parker	71295SN2KNJ1N0C111P3	n/a	120 VAC	Nitrogen fuel line purge	10.34 bar (150 psig)	10 Watt max
Hoerbiger	PD43295-5733	n/a	120 VAC	UCI fuel valve control	10.14 bar (147 psig)	6.9 VA max
UCI	N4S-D1	n/a	120 VAC	UCI rig air valves control	n/a	6.0 VA max
Thermocouple	Model	Serial #	Range	Use	Accuracy	Temperature Limits
Omega	KMQSS-125U-6 and 062U-6 type K	n/a	-6.458 to 54.886 mV	Temp point measurments in system	±4 F or 0.75%	-234 to 1372 °C (-454 to 2501 °F)

Appendix B: Operational Checklist for System Startup

Make sure the "Equip" control switch at the control station is in the OFF position before system startup, this must be on after the VI is started

To start up the laboratory equipment, turn ON the following:

1. Computer
2. Power switch on surge protector (powers DC supplies, SCXI 1100 and DAQPad 6508)
3. Instrument airline (note: another valve is located in Room 256)
    a. Check pressure control valve to IPT^2 reads 20-40 psi
    b. Check pressure control valve to other equipment reads 80 to 120 psi
4. ISCO fuel pump

Next, do the following:

1. Open and START Combustion Lab VI on computer
2. Check that relays are responding to operation of VI controls
    a. If this fails try stopping and restarting the VI and the DAQPad6508
    b. If step 2a fails then restart computer
3. Turn ON the "Equip" switch and check proper operation of all valves
    a. Set all valves to OFF position before proceeding
4. Turn on California Analytical Instruments gas analyzer
    a. Check that the VI readings match the analyzer displays

Check the following:

1. Emissions temperature control is set to 340°F at control station
2. Emissions temperature control is set to 350°F at gas analyzer
3. Emissions filter is set to 200°F at gas analyzer
4. Pressure, temperature and humidistat readings are reasonable
5. Temperature setting for airline heaters is below 500°F

For ignition do the following:

1. Turn on the exhaust system
2. Turn ON the gases to combustor stand
    a. Nitrogen
    b. Zero Air
    c. Ethylene (C_2H_4)

3. Turn ON the Mokon oil system – PROBE MUST BE IN DESIRED POSITION AND THERMOCOUPLE CONNECTED
    a. Open bypass valve at heater
    b. Check temperature is set to 350°F
    c. Check discharge pressure is near but below 40 psi
    d. Ensure that chiller lines are open
    e. Power ON
    f. When fluid is to temperature, close bypass valve and recheck all settings
    g. Check temperature for probe oil temp is near 350°F in VI
4. Check that all valves are OFF at VI
5. Turn ON air heaters (temp setting must be below 500°F)
6. Set rig airline flow to rate for ignition
7. Open manual fuel line valve at combustor stand
8. Set fuel flow rate or pressure for ignition in VI
9. Turn ON probe purge at VI
10. Turn ON air valves at VI
11. Turn ON ethylene and air valves at VI
12. Turn ON ignition switch at VI
13. Check torch is ignited
14. Turn OFF ignition switch at VI
15. Turn ON fuel valve at VI
16. Turn ON fuel pump switch at VI
17. Check ignition has occurred
18. Turn OFF ethylene and air valves
19. Change air and fuel flow to desired settings
20. Proceed with experiment

Bibliography

AIAA Optical Diagnostics Reference Sheet, AIAA website, 23 January 2006. www.aiaa.org/tc/amt/techniques.html

Anisko, J. (2006). Numerical investigation of cavity-vane interactions within the ultra compact combustor. (Master's thesis, Graduate School of Engineering, Air Force Institute of Technology (AU), Wright-Patterson AFB OH, March 2006). (AFIT/GAE/ENY/06-M01)

Anthenien, R. A., Mantz, R. A., Roquemore, W. M., & Sturgess, G. (2001). Experimental results for a novel, high swirl, ultra compact combustor for gas turbine engines. *2nd Joint Meeting of the United States Section of the Combustion Institute,* Oakland, CA.

Benard, P. S., & Wallace, J. M. (2002). *Turbulent flow: Analysis measurement and prediction*. Hoboken, NJ: John Wiley & Sons Inc.

California Analytical Instruments. (2003). *Model 400 HCLD instruction manual*. Orange, CA:

California Analytical Instruments. *Model 300 HFID/MHFID (CE version) heated hydrocarbon analyzer instruction manual*. Orange, CA:

California Analytical Instruments. *Operation and maintenance manual for infrared analyzers models 100, 200, 300*. Orange, CA:

California Analytical Instruments. *Supplemental oxygen manual for models 100, 200, 300 analyzers*. Orange, CA:

Dittman, E. R. (2006). Design, build and validation of a small scale combustion chamber testing facility. (Master's thesis, Graduate School of Engineering, Air Force Institute of Technology (AU), Wright-Patterson AFB OH, March 2006). (AFIT/GAE/ENY/06-M06)

Eckbreth, A. C. (1988). In Gupta A. K., Lilley D. G. (Eds.), *Laser diagnostics for combustion temperature and species* (1st ed.). Tunbridge Wells, Kentucky: Abacus Press.

Eckbreth, A. C., Bonczyk, P. A., & Verdieck, J. F. (1979). Combustion diagnostics by laser raman and fluorescence techniques. *Progress in Energy and Combustion Science, 5*, 253-322.

Eckbreth, A. C., & Stufflebeam, J. H. (1988). CARS diagnostics for combustion and plasma processes. *Materials Research Society Symposium, Process Diagnostics: Materials, Combustion, Fusion,* Reno, NV. *, 117* 217-226.

Greenwood, R. T. (2005). Numerical analysis and optimization of the ultra compact combustor. (Master's thesis, Graduate School of Engineering, Air Force Institute of Technology (AU), Wright-Patterson AFB OH, March 2005). (AFIT/GAE/ENY/05-M10)

Lewis, G. D. (1973). Swirling flow combustion -- fundamentals and application. *AIAA/SAE 9th Propulsion Conference,* Las Vegas, Nevada.

LIFBASE website, Jorge Luque, 22 February 2007. http://www.sri.com/psd/lifbase/

Liu, F., & Sirignano, W. A. (2000). Turbojet and turbofan engine performance increases through turbine burners. *38th Aerospace Sciences Meeting and Exhibit,* Reno, NV.

Meyer, T. R., Roy, S., Belovich, V. M., Corporan, E., & Gord, J. R. (2005). Simultaneous planar LII, OH PLIF, and droplet mie scattering in swirl-stabilized spray flames. *Applied Optics, 44*(3), 445-454.

Moenter, D. S. (2006). Design and numerical simulation of two-dimensional ultra compact combustor model sections for experimental observation of cavity-vane flow interactions. (Master's thesis, Graduate School of Engineering, Air Force Institute of Technology (AU), Wright-Patterson AFB Ohio, September 2006). (AFIT/GAE/ENY/06-S07)

Quaale, R. J., Anthenien, R. A., Zelina, J., & Ehret, J. (2003). *Flow measurements within a high swirl ultra compact combustor for gas turbine engines* No. ISABE-2003-1141)

Roquemore, W. M., Shouse, D., Burrus, D., Johnson, A., Cooper, C., & Duncan, B., et al. (2001). Trapped vortex combustor concept for gas turbine engines. *39th AIAA Aerospace Sciences Meeting & Exhibit,* Reno, NV. 1.

Roy, S., Meyer, T. R., Lucht, R. P., Belovich, V. M., Corporan, E., & Gord, J. R. (2004). Temperature and CO2 concentration measurements in the exhaust stream of a liquid-fueled combustor using dual-pump coherent anti-stokes raman scattersing (CARS) spectroscopy. *Combustion and Flame, 138*, 273-284.

Vander Wal, Randall L. (1997). *Using laser-induced incandescence to measure Soot/Smoke concentrations* No. NASA/CR-97-206325)NASA Lewis Research Center.

Wainner, R., & Seitzman J. M. (1997). Simultaneous measurement of soot properties by laser-induced incandescence. *35th AIAA Aerospace Sciences Meeting & Exhibit,* Reno, NV.

Wilson, D. G., & Korakianitis, T. (1998). *The design of high-efficiency turbomachinery and gas turbines* (2nd ed.). Upper Saddle River, New Jersey: Prentice Hall.

Yonezawa, Y., Toh, H., Goto, S., & Obata, M. (1990). Development of the jet-swirl high loading combustor. *AIAA/SAE/ASME/ASEE 26th Joint Propulsion Conference,* Orlando, FL.

Zelina, J., Shouse, D. T., & Neuroth, C. (2005). High pressure tests of a high-g ultra-compact combustor.

Zelina, J., Sturgess, G. J., Manour, A., & Handcock, R. D. (2003). *Fuel injector design for an ultra-compact combustor"* No. ISABE-2003-1141

Zelina, J., Sturgess, G. J., & Shouse, D. T. (2004). The behavior of an ultra-compact combustor (UCC) based on centrifugally-enhanced turbulent burning rates.

REPORT DOCUMENTATION PAGE

Form Approved
OMB No. 074-0188

1. REPORT DATE *(DD-MM-YYYY)*	**2. REPORT TYPE**	**3. DATES COVERED** *(From – To)*
22 Mar 07	**Master's Thesis**	Oct. 2006 – Mar. 2007

4. TITLE AND SUBTITLE

DESIGN, CONSTRUCTION, AND VALIDATION OF THE AFIT SMALL SCALE COMBUSTION FACILITY AND SECTION MODEL OF THE ULTRA-COMPACT COMBUSTOR

5a. CONTRACT NUMBER

5b. GRANT NUMBER

5c. PROGRAM ELEMENT NUMBER

6. AUTHOR(S)

Anderson, Wesly S., 2nd Lt, USAF

5d. PROJECT NUMBER

5e. TASK NUMBER

5f. WORK UNIT NUMBER

7. PERFORMING ORGANIZATION NAMES(S) AND ADDRESS(S)
Air Force Institute of Technology
Graduate School of Engineering and Management (AFIT/EN)
2950 Hobson Way
WPAFB OH 45433-7765

8. PERFORMING ORGANIZATION REPORT NUMBER

AFIT/GAE/ENY/07-M01

9. SPONSORING/MONITORING AGENCY NAME(S) AND ADDRESS(ES)

AFRL/PRS	AFRL/PRTC
Michael Huggins	Dr. Joseph Zelina
5 Pollux Dr.	1950 Fifth Street
Edwards AFB, CA 93524-7680	WPAFB, OH 45433-7251

10. SPONSOR/MONITOR'S ACRONYM(S)

11. SPONSOR/MONITOR'S REPORT NUMBER(S)

12. DISTRIBUTION/AVAILABILITY STATEMENT
APPROVED FOR PUBLIC RELEASE; DISTRIBUTION UNLIMITED.

13. SUPPLEMENTARY NOTES

14. ABSTRACT

The AFIT small-scale combustion facility is complete and its first experiment designed and built. Beginning with the partially built facility, detailed designs have been developed to complete the laboratory in order to run small-scale combustion experiments at atmospheric pressure. A sectional model of the Ultra-Compact Combustor has also been designed and built. Although the lab's specific design intent was to study the UCC's cavity-vane interaction, facility flexibility has also been maintained for future work. The design enabled the completion of liquid fuel and air delivery systems, power and control systems, and test equipment. The design includes failsafe operation, remote control, and adherence to SAE ARP 1256 testing standards. Construction of the laboratory has forced design changes as new obstacles arose. As system construction has been completed validation and troubleshooting have been undertaken. The AFIT facility can now deliver air in two separately controlled air lines at up to 530 K (500 °F), at delivery rates of 0.12 kg/s (200 SCFM) for the main line and 0.03 kg/s (60 SCFM) for the secondary. A continuous dual syringe pump can deliver liquid fuel at up to 5.67 mL/s for JP-8 equivalence ratios up to 4. Safe, remote ignition and shutdown are in place and all test equipment fundamental to combustion is installed. The addition of an advanced laser combustion diagnostics system adds more unique capability to the laboratory. The laser system will provide instantaneous Raman and Raman spectroscopy, Coherent Anti-Stokes Raman Scattering, Planar Laser-Induced Fluorescence, Laser-Induced Incandescence and Planar Imaging Velocimetry diagnostic techniques.

15. SUBJECT TERMS
Combustion, Combustors, Design, Emissions, Experimental, Laboratory, Laser Diagnostics, Ultra-Compact Combustor

16. SECURITY CLASSIFICATION OF:			**17. LIMITATION OF ABSTRACT**	**18. NUMBER OF PAGES**	**19a. NAME OF RESPONSIBLE PERSON**
REPORT	**ABSTRACT**	**c. THIS PAGE**			Major Richard Branam, ENY
U	**U**	**U**	**UU**	113	**19b. TELEPHONE NUMBER** *(Include area code)* (937) 255-3636 x7485,

Standard Form 298 (Rev: 8-98)
Prescribed by ANSI Std. Z39-18